AALBORG UNIVERSITY
DENMARK

Strength and Deformation Properties of Preconsolidated Moraine Clay

Jacobsen, Moust

Published in:
Bulletin No. 27

Publication date:
1970

Document Version
Publisher's PDF, also known as Version of record

Link to publication from Aalborg University

Citation for published version (APA):
Jacobsen, M. (1970). Strength and Deformation Properties of Preconsolidated Moraine Clay. In *Bulletin No. 27* (pp. 21-45). The Danish Geotechnical Institute.

Strength and Deformation Properties of Preconsolidated Moraine Clay

Moraine Clay

The glacial till has been deposited by the inland ice moving from the Scandinavian mountains. It is normally an unsorted material containing blocks (reaching half a metre in diameter), gravel, sand, silt and clay, all mixed together. Some of it was transported in the deeper part of the ice sheet and deposited under great pressure, forming a very solid and compact soil. Some of it was situated in the upper part of the ice, gradually appearing on the surface as the ice melted and thus forming a rather loose deposit in a thin superficial layer (ablation moraine). All nuances exist, from the heavily overconsolidated till to the ablation moraine.

The till is called moraine clay (or boulder clay), moraine sand or moraine gravel, according to the grain-size distribution of the material.

Moraine clay contains 15–50 % clay fraction. The lower limit is set by the geotechnical requirement that it should be possible for undrained circumstances to occur, the upper limit is set by the geological requirement that the grain composition should be well graded. The upper limit may thus be rather indefinite.
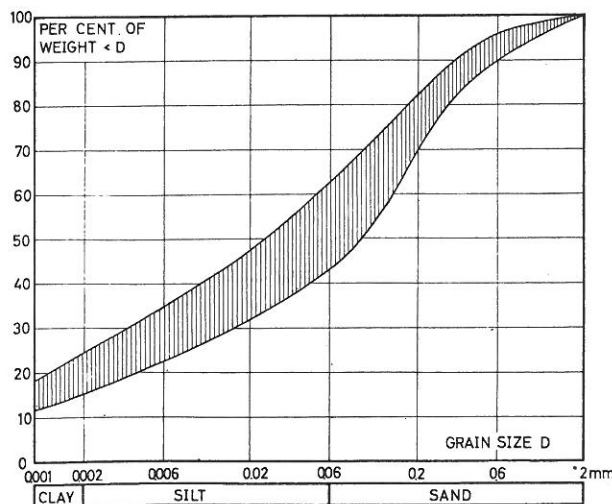
Some moraine clay deposits may be locally rather homogeneous, which means that the grain composition and the void ratios vary only little within a small area. By making field tests and by sampling within this area it is possible to make valid comparisons between laboratory tests and field tests. All tests mentioned here are carried out under these circumstances.

This paper deals with seven kinds of moraine clay, covering nuances from a very stiff moraine clay to a weak one, and having undrained shear strengths varying from 5–70 t/m². The variation in grain-size distribution is shown in fig. 2.1. The content of sand fraction is 40–60 %, of silt 25–50 % and of clay 15–25 %. The unweathered moraine clays contain 13–23 % calcite, a weathered one only 0.5 %. It will be shown that the moraine clays under consideration can be treated as one type of soil, but with varying voids ratios.

The results of classification tests are given in table 2.1. Here is also given a short geological description of the soils. The void ratio given in column 1 is suffixed by k. It is ascertained by the so-called bulk density method, in which the volume of a lump of clay is determined by submerging it in trichlorethylene. The normal method is to cut off a cylindrical sample, weigh it wet and dry and calculate the volume, the water content and the void ratio. The surface of a moraine clay sample is not smooth, stones placed in the surface make it rough and the volume determination rather doubtful. Therefore the measured strength properties will be compared on the basis of e_k.

The water content calculated in the normal way corresponds to a degree of saturation of 85–95 % only. This is due to the low capillarity of a boulder clay. Measurements show that for a normal moraine clay the capillarity is less than 10 t/m², except in the heaviest overconsolidated moraine clays. This means that when the overburden pressure is greater than the capillarity pressure the pore water suction during

Fig. 2.1 Grain size distribution of the moraine clays here treated.

TABLE 2.1
Types of moraine clay

Locality	e_k	$w\ ^0/_0$	Consistency limits		$CaCO_3$ $^0/_0$	Geological description
			$w_L\ ^0/_0$	$w_P\ ^0/_0$		
Sabro	0.52	19.2	27.5	13.7	0.5	Moraine clay, rather silty, sand contents rather fine, weathered and soft.
Amager	0.36	13.4	–	–	–	Moraine clay.
Odense (profile)	0.31	11.4	19.6	10.1	23	Moraine clay, stoney, sandy, sligthly cemented.
	0.25	9.1	20.3	9.9	16	Moraine clay, stoney, sandy.
	0.26	9.7	17.8	11.4	58	Moraine clay, rich in calcite, stoney.
Carlsberg II	~ 0.30 ~ 0.36	–	19.9	11.1	–	Moraine clay, unweathered.
Kratbjerg	0.32	12.0	17.9	10.8	18	Moraine clay, sand contents rather fine.
Odense IV	0.32	12.0	20.0	9.8	20	Moraine clay, stoney, sandy.
Carlsberg I	0.24	9.0	20.9	10.6	13	Moraine clay, sandy, stoney, extremely hard, rather cemented, dark grey, unweathered.

sampling can only increase to this amount. Air will enter through some sandy canals in the sample. During preparation the sample will dry somewhat and more air enter in the same way. In the table the natural water content is given corresponding to fully saturated soils.

Strength Properties

Investigations of the deformation properties of moraine clay were carried out at the Danish Geotechnical Institute as part of the author's thesis for the technical licentiate degree. During this work some other results were obtained, such as construction of new triaxial apparatus and oedometers, and measurements of strength properties in plate loading tests, vane tests and laboratory tests.

These tests are not primarily carried out as failure tests, and therefore for some of the moraine clays mentioned in this paper relatively few tests are treated, while for other moraine clays the test material is fairly extensive. Table 2.2 gives a summary of the different test types and the numbers of tests dealt with in this paper.

Test procedures
Laboratory tests
Our laboratory tests consist of undrained compression tests and undrained and drained triaxial tests performed on cylindrical samples with a diameter equal to the height.

TABLE 2.2
Test types and numbers of tests

Locality	vane tests	Undrained plate tests	Unconfined compression tests	Drained plate tests	Triaxial tests $CU, u = 0$	Triaxial tests CD
Sabro	x	6	–	5	5	–
Amager	x	–	16	–	–	–
Odense	x	–	–	–	3	–
Carlsberg II	x	2	–	6	3	–
Kratbjerg	x	–	8	16	6	8
Odense IV	x	–	–	–	–	–
Carlsberg I	x	6	2	1	3	–

In the tests mentioned here, new triaxial equipment with smooth pressure heads was used as described in the first paper. A test series was made to check up on

the effect of the "smooth" pressure heads, showing that the influence of the remaining roughness is negligible when using samples with the height equal to the diameter. This has been described earlier.

Samples used in our triaxial tests had a cross section area of 38.5 cm² and a height of 7 cm. Those used in unconfined compression tests had a cross section of 10 cm² and a height of 3.6 cm. The samples were normally taken from block samples with a diameter and height of 15 cm.

When sampling in the normal way some disturbance might perhaps occur, creating cracks in the sample and thus causing errors. This is prevented by use of hand-cut block samples, even for heavily overconsolidated clays.

Field tests

Our field tests consist of vane tests, and undrained and drained loading tests with circular plates.

The vane tests were carried out by means of the vane ordinarily used by the Danish Geotechnical Institute. Normally the duration of a test is shorter than one minute in order to avoid drainage of water to the enforced rupture surface. Usually moraine clay expands under rupture, and the pore water suction in the rupture surface causes a great part of the undrained shear strength. Therefore, if tests are made more slowly, a tendency towards smaller values of c_v will appear.

Stones in the rupture surface cause grave errors. Mostly the stones cause jerks in the movements of the vane. These tests are of course rejected. In an enforced surface even small stones will make the shear strength c_v exceed that of the soil proper.

Plate tests are normally carried out with circular plates which have diameters between 5 and 30 cm and which are loaded vertically. The test area is as plane as possible and has a diameter of at least 5, normally 7 times the diameter of the plate. The plate is placed where no stones appear in the soil surface, and gypsum or concrete is cast between the plate and the soil surface. After the test the soil under the plate is dug out to investigate stones under the plate, possibly influencing the test results.

The test areas are normally situated above the ground water level and the tests are carried out so long after excavation that the actual overburden pressure in the soil under consideration is nearly effective. In order to determine this pressure it is necessary to know the amount of pore water suction caused by the capillary forces acting as a surface load. This can be done in two different ways, either by flooding the test areas in order to decrease the suction to zero, or by measuring the suction. The first method causes swelling of the soil during a very long period and at the end of this period the void ratio has changed very much, altering the strength properties considerably. The second method is of course preferable but it requires pore water suction measuring equipment. When making undrained plate tests the effective overburden pressure is of minor importance as mentioned later. In these tests it is not determined in all cases.

The device for measuring pore water suction consists of a spike with filters at the end, a screw-controlled plunger and a mercury manometer as seen in fig. 2.2. First the system is filled with water and mercury by means of the plunger. It is important to avoid air bubbles in the system. The spike is hammered into
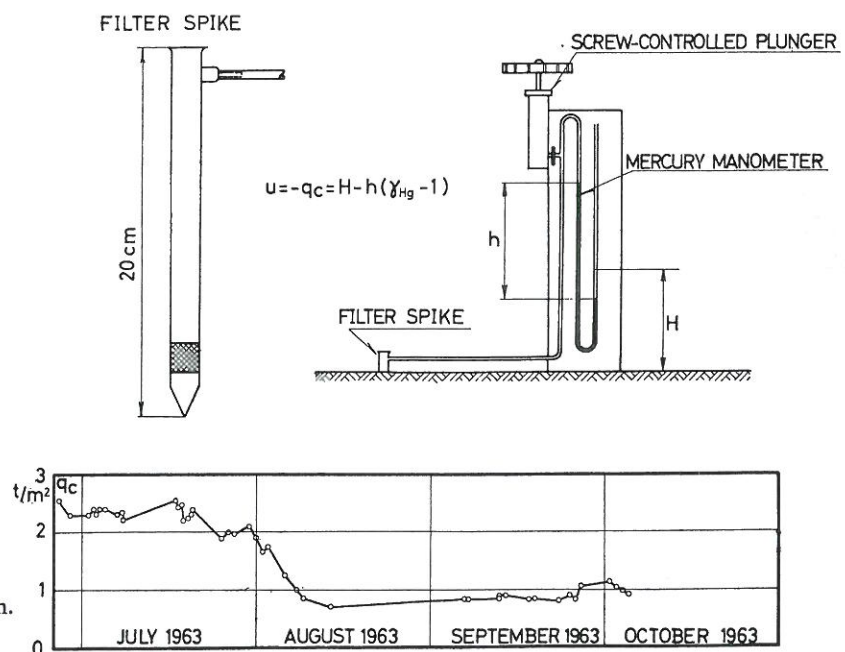

$$u = -q_C = H - h(\gamma_{Hg} - 1)$$

Fig. 2.2 Pore water suction measuring system. Example of observations.

the soil while water flows out of the filter to avoid air between the spike and the soil. Afterwards the soil is compacted near the spike in order to close fissures in the soil. Now the water flows from the manometer into the soil through the spike. After 8 hours the flow stops, indicating that the suction in the soil corresponds to the suction in the manometer.

This system is calibrated in the laboratory and shows very good results within the range normally used (0–2.5 t/m²). In fig. 2.2 is also shown some observations. It will be seen that in August and September, which were very rainy months, the ground water level was raised nearly two metres.

Evaporation from the surface of the test area also causes suction in the pore water, varying very much with the temperature at the soil surface. In order to prevent this, the test area is covered with a thin layer of sand.

An additional surface load can be applied by covering the test area with a thicker layer of sand or a layer of sand loaded with steel bars. It is necessary to let the moarine clay consolidate before the test to obtain measurement of the effective strength parameters. In this way it is difficult to get an exact measurement of the settlement of the plate. In some tests an additional sand load combined with a neutralizing of pore water suction can give further control of the pore water suction.

The tests are normally performed as controlled strain tests. The vertical load is applied by means of a hydraulic jack or a screw spindle. The load is measured by a loading cell directly in connection with the plate. Undrained tests have a duration of less than one hour, while drained tests last about a week.

During tests the plates sometimes tilt or move sidewards (fig. 2.3). Owing to the test arrangement this
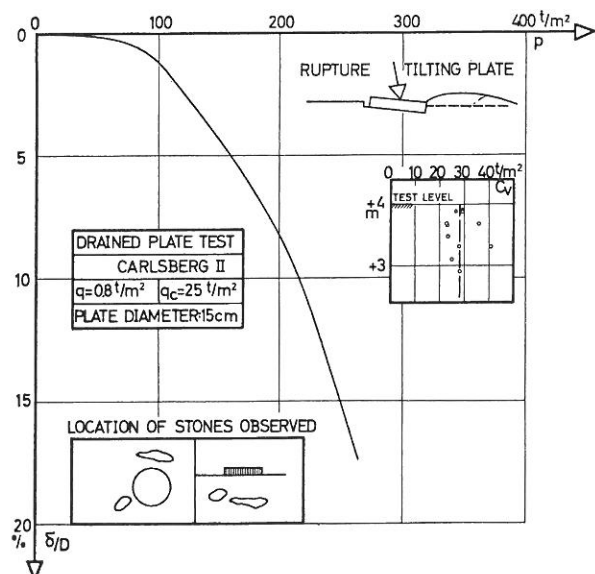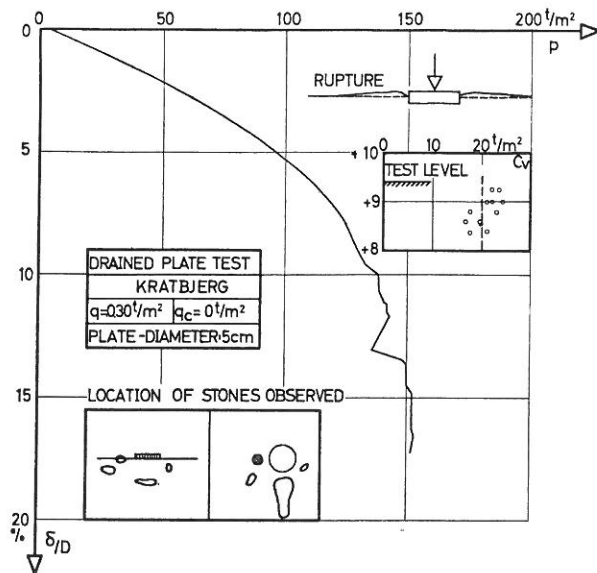

Fig. 2.4 Drained plate test with a distinct failure load. Results of vane tests c_v are also shown.

gives a horizontal component of the applied load on the plate. This causes a different shape of the performance curve from that in a test with an untilted plate (fig. 2.4). The difference is due to that fact that untilted plates give maximum values of the plate load, sometimes as peak points, whereas tilted plates give slightly increasing plate loads when the plate is pressed down into the soil. Untilted plates normally give a well-defined ultimate bearing capacity, whereas it is difficult to give a consistent failure definition for tilting plates.

Undrained shear strength

The undrained shear strength can be determined from triaxial tests, unconfined compression tests, plate loading tests or vane tests.

The most appropriate method of measuring the strength is to perform plate tests direct on the soil surface. In this way the soil is nearly undisturbed, if it is carefully smoothed. The short-term ultimate bearing capacity can be found from

$$p_f = c_u^p \cdot s_c^o \cdot N_c^o + \bar{q}$$

Taking $N_c^o = \pi + 2$, $s_c^o = 1.2$ and ignoring the surface load $\bar{q}$, which is of minor importance, we get:

$$c_u^p = p_f/6.2$$

The effective surface load does not include pore pressures in the undrained state, because these also act under the plate and therefore have the same effect on both sides of the equation.

The result of an undrained plate test is shown in fig. 2.5.

Fig. 2.3 Drained plate test with tilting of the plate. The failure load cannot be determined without a specific definition.
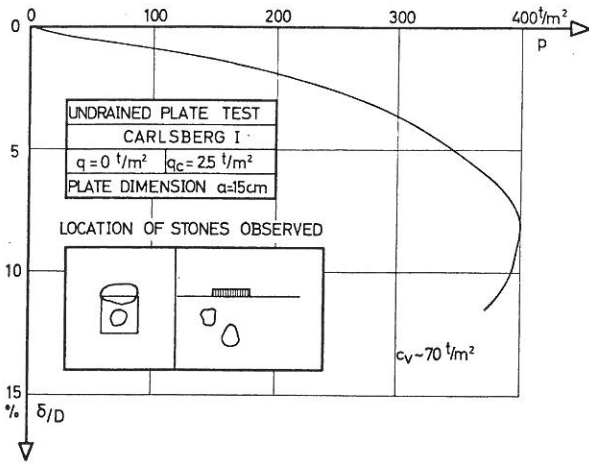
Fig. 2.5 Undrained plate test.

In some of the laboratory tests the formation of radial cracks transforms the sample into a series of smaller specimens with $H > D$. These tests show maximum deviator stress as a peak point, like tests with a height twice the diameter influenced by the formation of a distinct rupture surface. In these tests the measured undrained shear strength corresponds to a higher water content than that measured, giving less shear strength (in mean only 40 %). Thus tests with radial cracks after failure have to be rejected. In the best laboratory tests the samples retain their cylindrical shape even after a vertical deformation of 30 %.

The shear strength is determined as

$$c_u = \frac{1}{2} (\sigma_1 - \sigma_3)_f$$

In vane tests the shear strength is measured in a vertical shear plane, whereas in laboratory tests the shear plane is inclined and in plate loading tests variable. A test series of unconfined compression tests performed with different inclinations of the axis seems to show that the influence of the orientation of the shear planes is negligible.

Consequently a comparison of different kinds of tests should be relevant.

This shows first of all that the agreement between results from vane tests c_v and plate tests c_u^p is quite good, if it is taken into account that c_v is measured in an enforced rupture surface. The average value is

$$c_u^p = 0.90 \, c_v$$

found in 14 tests. The standard deviation of the constant is 0.02.

A comparison between vane tests and unconfined compression tests gives

$$c_u = 0.93 \, c_v$$

found in 14 tests. The standard deviation is 0.035.

There is no statistical reason to distinguish between c_u and c_u^p, but the vane tests give a somewhat higher value, nearly 10 %.

Consequently, when using the results of vane tests we have to reduce the vane strength by 10 % in order to get the actual undrained shear strength.

These results are shown in table 2.3 and fig. 2.6. It

TABLE 2.3
Undrained shear strength c_u (t/m²)

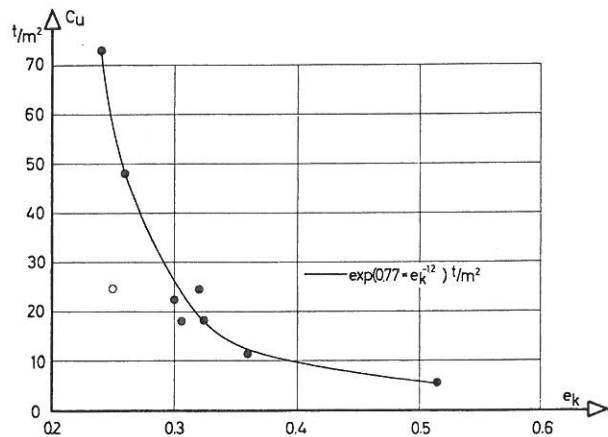| Locality	e_k	Plate tests c_u^p	Unconfined compression tests c_u	Vane tests c_v	Numbers of tests
Sabro	0.52	5.35	–	5.75	6
Amager	0.36	–	11.3	13	16
Odense I	0.31	–	–	20	–
	0.25	–	–	28 (?)	–
	0.26	–	–	53	–
Carlsberg II	0.30	19.4	–	25	2
Kratbjerg	0.32	–	18.3	20	8
Odense IV	0.32	–	–	27	–
Carlsberg I	0.24	75	73	70	6+2

Fig. 2.6 The undrained shear strength versus void ratio e_k.

will be seen that the results can be represented by one curve, giving the undrained shear strength as a function of the void ratio:

$$c_u = \exp (0.77 \cdot e_k^{-1.2}) \text{ t/m}^2 \qquad (2.1)$$

If this curve is used on the basis of void ratios measured in the normal way, it gives conservative estimates of the shear strength.

Triaxial tests give the same results as unconfined compression tests, but here the influence of the stress history can be investigated and a very good method to find the preconsolidation pressure can be employed.

Undrained triaxial tests consist of two parts. First, a consolidation of the sample at an isotropic pressure $\bar{\sigma}_{3,c}$. After this follows the undrained part of the test, giving the undrained shear strength $c_u = \frac{1}{2}(\sigma_1 - \sigma_3)_f$.

If a normally consolidated clay is tested we find that c_u is proportional to $\bar{\sigma}_{3,c}$:

$$c_u = k_u \cdot \bar{\sigma}_{3,c} \qquad (2.2)$$

In glacial times ice loads consolidated the moraine clay at a certain pressure, not isotropic, but corresponding to an isotropic pressure $\bar{\sigma}_{3,pc}$, giving the soil a shear strength $c_{u,pc}$. When the ice melted, the soil was unloaded, and the shear strength decreased, first very slightly, for smaller pressures more and more, as illustrated in fig. 2.7 until $\bar{\sigma}_{3,0}$, the mean normal stress corresponding to the in situ overburden pressure. If some disturbance occurs during sampling, the mean normal stress corresponding to the condition of the sample in the laboratory is less than $\bar{\sigma}_{3,0}$. Let us assume that no disturbance occurs.

Fig. 2.8 The effect of stress history measured on a Sabro moraine clay. It can be seen that there is good agreement between the undrained shear strength and the vane strength ($c_u \sim 0.9\ c_v$).
This means that the reconstruction of stress history is correct.

exceeding $\bar{\sigma}_{3,pc}$ without unloading the constant k_u in equation (2.2) can be determined. In this way we found for Sabro moraine clay $k_u = 0.5$ (fig. 2.8), $\bar{\sigma}_{3,pc} = 12$ t/m² and $c_u = 5.9$ t/m², for Kratbjerg moraine clay with $c_u = 18$ t/m² we got $\bar{\sigma}_{3,pc} \sim 40$ t/m² and for Carlsberg I moraine clay with $c_u \sim 60$ t/m² we found $\bar{\sigma}_{3,pc} \geq 100$ t/m², which means $k_u = 0.45$ and 0.6.
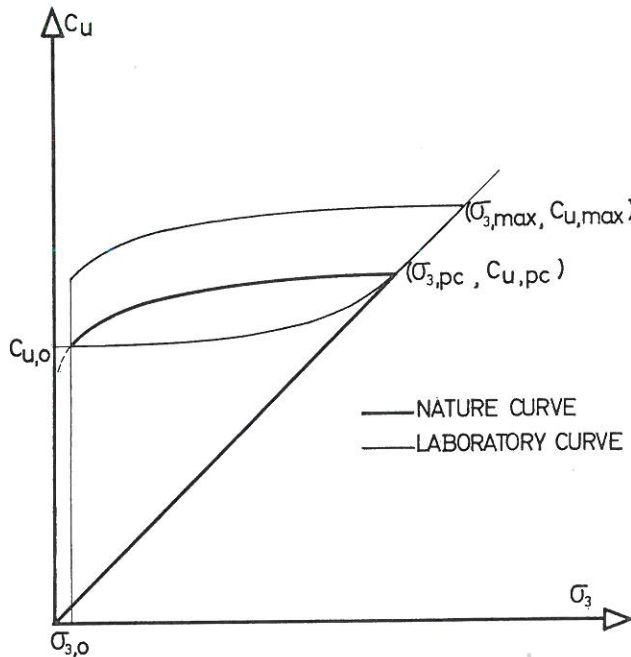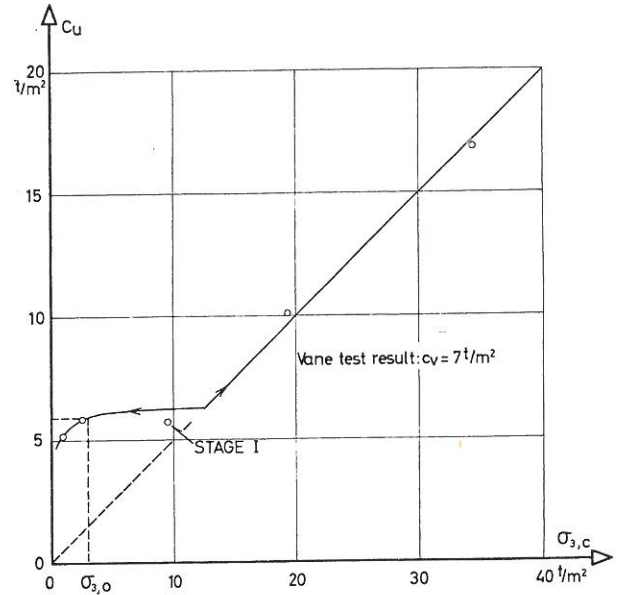
The most probable value of k_u is thus $k_u = 0.5$.

Fig. 2.7 The effect of stress history, here represented by σ_3, on the undrained shear strength.

During the first part of the triaxial test c_u will increase due to increase of $\bar{\sigma}_3$, at the beginning only slightly. The maximum mean normal stress in the laboratory is called $\bar{\sigma}_{3,max}$.

When unloading from this value we should get a curve similar to that in nature. After unloading to $\bar{\sigma}_{3,0}$ the undrained shear strength is measured. We have already the in situ shear strength of the soil $c_{u,0}$ measured by means of the vane or in unconfined compression tests. By comparing $c_{u,0}$ with that measured in the triaxial test we can see whether $\bar{\sigma}_{3,max} \sim \bar{\sigma}_{3,pc}$ or not. If not, another test can be made. When

Effective Strength Properties, Measured in The Field

Moraine clay is preconsolidated, thus having both effective cohesion and effective friction. The strength properties can be measured in the laboratory by triaxial tests as well as in the field by plate loading tests.

Plate loading tests

In the field plate loading tests of long duration can be performed, but this requires an accurate knowledge of the effective stress level. The plates are circular, vertically and centrally loaded and are at the beginning of the test located at the surface of the soil. Using the formula for bearing capacity as given by Brinch Hansen (1961):

$$p_f = 1/2\ \bar{\gamma}\ BN_\gamma s_\gamma d_\gamma i_\gamma + \bar{q}N_q s_q d_q i_q + \bar{c}N_c s_c d_c i_c$$

we have $d_\gamma = i_\gamma = i_q = i_c = 1$ and $d_q \sim d_c \sim 1$. The shape factors are estimated to be: $s_\gamma = 0.6$ and $s_q = s_c = 1.2$.

This gives

$$p_f = \frac{1}{2}\overline{\gamma}\,D N_\gamma s_\gamma + \overline{q} N_q s_q + \overline{c} N_c s_c \qquad (2.3)$$

$\overline{q}$ is the effective surface load including capillary stresses q_c. Designating the applied surface load by q we have

$$\overline{q} = q_c + q$$

The plate diameters are normally small ($D < 0.3$ m) making the first part of (2.3) unimportant. This means that in a test series on moraine clay only one diameter is necessary:

$$p_f \simeq 1.2\,\overline{q}\,N_q + 1.2\,\overline{c}\,N_c$$

By comparing tests with different surface loads N_q can be calculated by means of the increase in p_f. From this $\overline{\varphi}_p$ can be determined and thus $N_c = (N_q - 1)\cot\overline{\varphi}_p$. By measuring the soil suction q_c, the real amount of surface load is ascertained and it is possible to determine $\overline{c}_p$.

The strength properties determined from plate loading tests are in this paper subscripted p in order to distinguish between plate test results and triaxial test results.

It can be shown that for low stress levels and swelling soils $\overline{c}$ decreases and $\overline{\varphi}$ increases so that the ultimate bearing capacity also reduces in accordance with the curved Mohr-envelope. This is appreciable for the tests under consideration, when the surface load is less than ~ 0.3 t/m². Therefore only tests with surface loads bigger than 0.3 t/m² will be treated here, giving a surface load interval of 0.3 — 3 t/m².

Locality: Kratbjerg

17 drained plate loading tests were carried out. One of these with controlled stress, the others with a rate of movement of $\dot{\delta}/D = 0.3$ % p.h., which appears to be the highest rate giving nearly drained circumstances. This was investigated in a special test series on Sabro moraine clay.

TABLE 2.4
Drained plate loading test

| Locality	Test no.	Plate diam. cm	q_c t/m²	q t/m²	$\overline{q}$ t/m²	p_f t/m²	
Kratbjerg	MS1	5	2.05		2.05	247	
	B3	5	1.0	1.0	2.0	257	
	B4	5		0.3	0.3	153	
	B5	5	0.85		0.85	175	
	B6	5	0.2		0.2	82	Swelling
	C4	5	1.2		1.2	218	
	C5	5	1.1		1.1	216	
	C6	5	1.05		1.05	231	
	C11	5	1.4		1.4	250	
	D5	15	~ 0		~ 0	<76	Swelling
	D6	15	~ 0		~ 0	<76	Swelling
	D10	5	0.8		0.8	179	
	D11	5	1.1		1.1	230	
	D12	5	0		0(?)	165	
	D13	5	0		0	106	Swelling
	E1	5	0	0.2	0.2	118	
	F2	5	0.45		0.45	107	Swelling
Carlsberg I	85	7.5	2.30	0	2.30	500	
Carlsberg II	87	7.5		0.35	0.35	90	
	1519	15	2.25		2.25	200	$c_v = 25$ t/m²
	1520	15		0.35	0.35	100	
	88	7.5		0.35	0.35	110	
	1518	15	2.25	0.80	3.05	260	$c_v = 28$ t/m²
	251	25		0.35	0.35	130	
Sabro	154	15	~ 0.1		~ 0.1	34.8	$c_v = 6.0$ t/m²
	155	15	~ 0.1		~ 0.1	45.0	$= 7.4$ t/m²
	156	15		0.77	0.78	59.0	$= 6.7$ t/m²
	158	15		0.78	0.78	41.0	$= 4.7$ t/m²
	301	30	~ 0.2		~ 0.2	35.6	$= 5.8$ t/m²
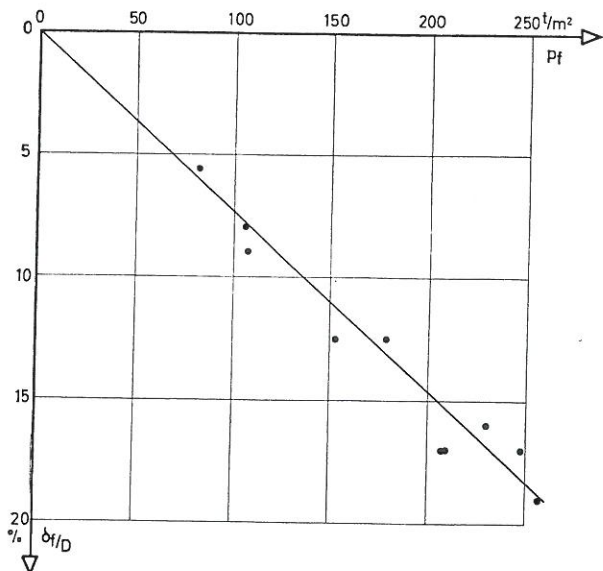
Fig. 2.9 Failure load p_f versus failure deformation δ_f. Plate tests on Kratbjerg moraine clay.

The test results are shown in table 2.4. Most of the tests show an ultimate bearing capacity p_f, and the corresponding deformation δ_f is also shown in the table. Fig. 2.9 shows that this deformation depends on the bearing capacity. In tests not showing maximum bearing capacities, owing to tilting of the plates, δ_f and p_f are determined by the intersection between this curve and the performance curve of the test.
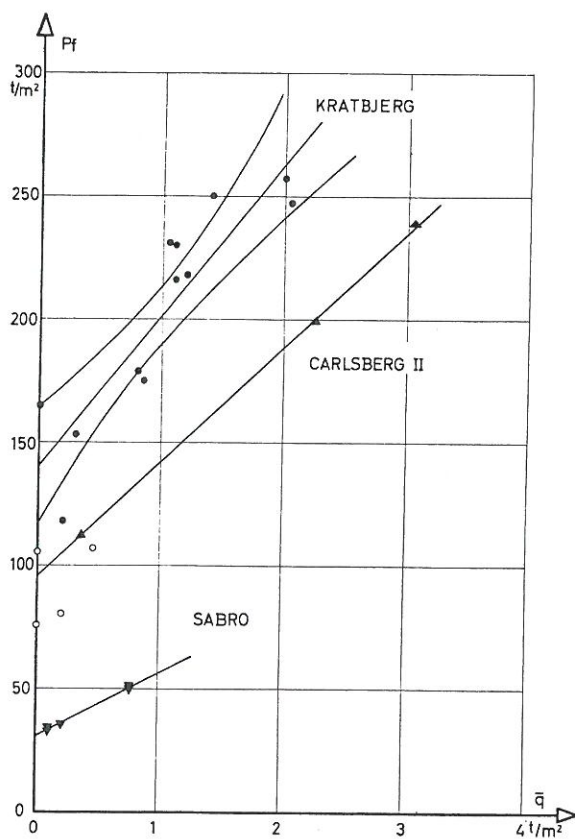

Fig. 2.10 Failure load p_f versus effective surface load $\overline{q}$. All plate tests are shown; in cases of swelling effects the points are shown transparent.

Normally the surface load mostly is due to soil suction. This depends on the weather, with decreases in rainy periods. Thus q_c varies during a test and the value of q_c in the table is that at the time of failure.

Six of the tests had surface loads less than 0.3 t/m². D11 gives too high a value of p_f, because the swelling period was only one hour.

Two tests, D5 and D6, were flooded during the test by mistake, giving a reduced $p_f \sim 76$ t/m².

Fig. 2.10 shows p_f as a function of $\overline{q}$. The straight line gives:

$$1.2\, \overline{c}_p N_c = 141 \text{ t/m}^2$$
$$1.2\, N_q = 61$$
$$N_q = 50.8 \text{ gives } \overline{\varphi}_p = 38°4$$
$$\overline{c}_p = 1.84 \text{ t/m}^2$$

Locality: Carlsberg

8 drained plate loading tests were carried out on two different types of moraine clay. Of these, two tests were performed on the very hard soil called Carlsberg I (table 2.4).

These tests illustrate the difficulties that arise from making the soil suction zero and applying surface loads. The soil suction device had just been constructed at this time but was not calibrated.

Four tests were made on Carlsberg II on two test areas with a surface load of 0.35 t/m² and with different plate diameters. Two of the tests give a difference in the two test areas. The results can be seen in fig. 2.11 showing the influence of the swelling zone. The limiting line lets p_f increase slightly with the diameter according to the γ-term of the formula 2.3. Two more tests were carried out with full suction in the soil. These tests are shown in fig. 2.11 together with the results from a plate of the same diameter with the swelling effect corrected. In one of the tests the differences in test areas were also corrected, namely by a difference in friction angle of about 1°.

In this way the following strength parameters were found

$$\overline{\varphi}_p = 36°2 \text{ and } \overline{c}_p = 1.56 \text{ t/m}^2 \text{ (Carlsberg II)}$$
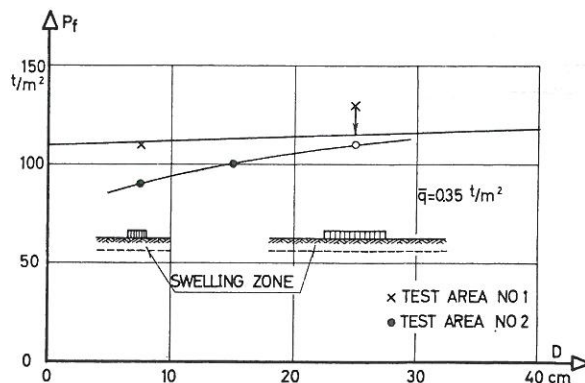

Fig. 2.11 The effect of swelling on the failure load influences the results as a scale effect. Plate tests on Carlsberg moraine clay.

On the hard soil Carlsberg I only one of the two tests was carried so far that a failure load could be predicted by use of the formula:

$$\frac{\delta}{\delta_f} = \frac{1}{4\,F^2 - 3}$$

given by Brinch Hansen and also used in three of the other tests. This of course only gives a relation between $\bar{c}_p$ and $\bar{\varphi}_p$.

Locality: Sabro

5 tests were carried out in order to calculate the influence of the rate of movement, this being $\dot{\delta}/D =$ 40 %, 7 %, 1.25 %, 0.3 % and 0.06 % p.h. The deformations in drained tests carried out with controlled stress should be the same as those in drained tests with the correctly chosen controlled strain. This shows that a strain rate of 0.3 % p.h. gives drained tests. When this result is used for other moraine clays, the limit rate of movement is not the same, owing to differences in permeability k, drainage path proportional to D, and a settlement modulus of the plate $K_p = \dfrac{p \cdot D}{\delta}$ t/m². By comparison we got the following general requirement:

$$\dot{\delta}/D < \frac{K_p \cdot k}{\gamma_w \cdot D^2} \cdot 10^{-2}\ \text{sec}^{-1}$$

All tests treated have fulfilled this requirement.

These tests are made on a level only 0.2 cm below ground water level, but without being flooded by water. This means that swelling of soil is avoided. When the shear strength varies from test to test, the ultimate bearing capacity is multiplied by $c_{u\,\text{mean}}/c_u$.

Fig. 2.10 shows the results of 5 plate tests with $c_u =$ 5.35 t/m² and the effective parameters are determined as:

$$\bar{\varphi}_p = 31°5 \quad \text{and} \quad \bar{c}_p = 0.75\ \text{t/m}^2$$

The figure also shows that the cohesion part of the long-term bearing capacity is 31 t/m² or nearly equal to the short-term bearing capacity being $6.2 \cdot 5.35 =$ 33 t/m².

Summary

The results can be correlated with the void ratio e_k. In spite of the fact that the number of tests is small, the variation of $\bar{c}_p$ and $\bar{\varphi}_p$ according to the void ratio is consistent (fig. 2.12). The only test on Carlsberg I also agrees with the other results. As the void ratio is known, fig. 2.12 gives $\bar{c}_p$, and the test result $\bar{\varphi}_p$, which gives a point on the upper curve.

These results make it possible to compare the short-term and long-term bearing capacities.

First we will consider the case of no surface load and D very small. A comparison between short-term
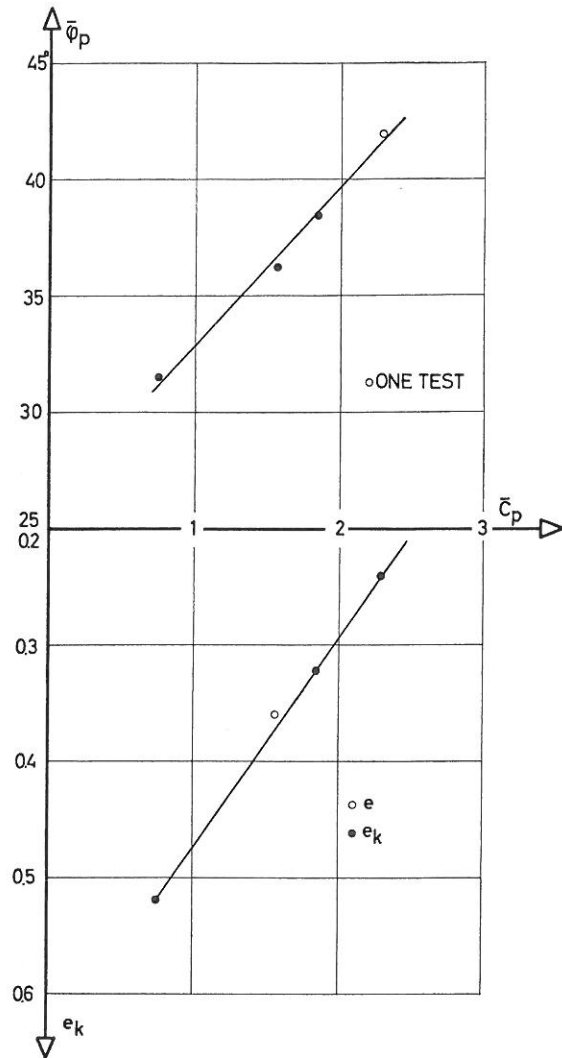

Fig. 2.12 Effective strength parameters $\bar{c}_p$ and $\bar{\varphi}_p$ determined by plate tests shown in fig. 2.9.

and long-term capacities gives the result shown in fig. 2.13. The black points represent the two test series on Kratbjerg and Sabro, the other points represent the results from Carlsberg and are rather uncertain. In the second figure, bearing capacities for increasing diameters (hatched) are shown in relation to the short-term bearing capacity and to the cohesion
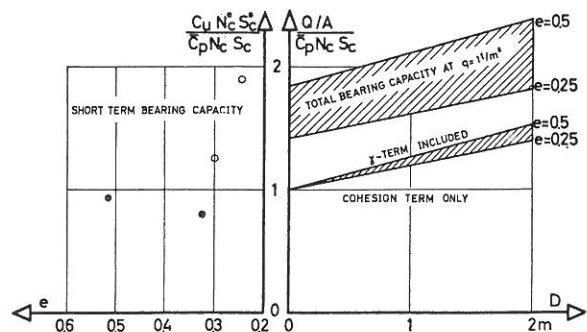

Fig. 2.13 A comparison between short-term and long-term bearing capacities as calculated by means of fig. 2.12.

29

part of the long-term bearing capacity. It will be seen that an approximation to formula 2.3 is

$$p_f = \bar{c}_p N_c s_c (1 + 0.2\,D) + \bar{q} \cdot N_q s_q$$

where D is inserted in metres and

$$\bar{c}_p N_c s_c \sim c_u N_c^o s_c^o \tag{2.4}$$

This gives as a main result that the long-term bearing capacity is greater than the short-term one, except perhaps for the most heavily overconsolidated clays.

Usually the bearing capacity is determined by measuring the vane strength c_v and by using a safety factor $f_c = 1.75$. This gives a real safety factor of 1.58 in the undrained state, but normally the construction period lasts long enough for the long-term conditions to be developed. This means that the total factor of safety is much bigger, e.g. for a circular footing with a diameter of 2 m, $F = 4$, even with a surface load of only 1 t/m².

This should be modified a little on account of the influence of the stress level as mentioned later. The modification is shown in fig. 2.14.
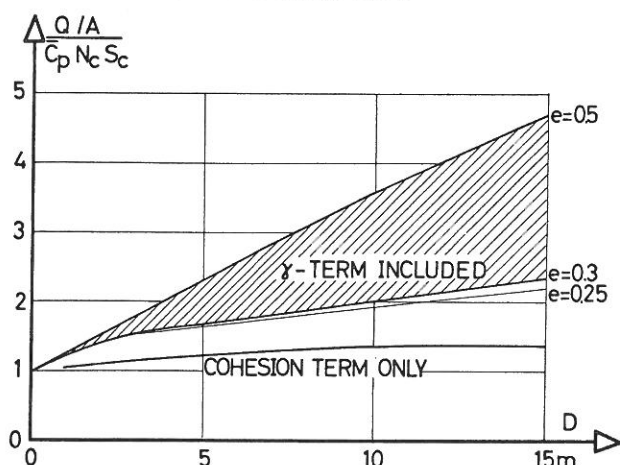

Fig. 2.14 The long-term bearing capacity modified on the basis of results of laboratory tests as mentioned in the conclusion.

The assumption made in 2.4 gives a check-up on some of the results. As an example the undrained shear strength will be calculated in two cases.

Example 1. $e > 0.3$

Fig. 2.12 gives for $e_k = 0.3$ the effective strength properties $\bar{c}_p = 2$ t/m² and $\bar{\varphi}_p = 39°4$. N_c is then found to be 70. c_u can be calculated from 2.4

$$c_u = \frac{2}{5.14} \cdot 70 = 27 \text{ t/m}^2.$$

Fig. 2.6 gives $c_u = 26$ t/m².

In the same way we get for $e_k = 0.4$, $c_u = 13$ t/m², and for $e_k = 0.5$, $c_u = 5.4$ t/m².

It is seen that there is sufficient agreement between measurements of short and long-term bearing capacities found by plate loading tests, and that assumption

(2.4) is nearly valid, at least when e_k is greater than 0.3.

Example 2. $e < 0.3$

Fig. 2.12 gives for $e = 0.25$, $\bar{c}_p = 2.3$ t/m² and $\bar{\varphi}_p = 41°2$. A calculation gives $c_u = 38$ t/m², whereas fig. 2.6 gives $c_u = 55$ t/m².

This means that for the smaller value of e the short-term bearing capacity is greater than the cohesion part of the long-term capacity, perhaps due to the suction in the soil, the amount of which increases with decreasing values of the void ratio. This tendency is also noted in fig. 2.13.

Effective Strength Properties Measured in Triaxial Tests

Triaxial tests have been performed both in a normal apparatus with a cross section area of the sample of 10 cm², the height being twice the diameter, and also in the new apparatus described in the first paper. It is thus possible to compare the results and in this way illustrate the amount of error.

If there are uniform stress and strain distributions throughout the sample, the shear strength τ_f in every part of the sample at failure is represented by Coulomb's equation:

$$\tau_f = \bar{c} + \bar{\sigma} \tan \bar{\varphi}$$

where the component $\bar{c}$ is called the cohesion and is independent of the normal pressure on the slip plane, whereas $\bar{\varphi}$ is the angle of internal friction.

The basic assumption is that $\bar{c}$ and $\bar{\varphi}$ are independent of the stress level, which means that the Mohr envelope is a straight line.

The most appropriate test on clay is the so-called $CU_{u=0}$ test. It is an undrained test but with open drains. The cell pressure is varied in such a way that the volume does not change during the test. The pore water pressure is zero and thus the effective stresses are measured. The results of this kind of test, then, give both the drained and undrained strength properties of a soil. In such a test the void ratio is kept constant and the performance curve has constant shear stresses at failure even at very large deformations, indicating that a remoulding effect apparently does not occur (fig. 2.15). This makes it possibles to perform several failure tests on the same sample, the so-called multiple-stages test (fig. 2.16). The first failure stage in a test of this kind normally gives a cohesion less than that measured later on, due to adaption of the sample to the pressure heads.

The stress history is reconstructed as far as possible. The first part of the test is an isotropic compression to a maximum pressure $\bar{\sigma}_{3,max}$, corresponding to the preconsolidation pressure $\bar{\sigma}_{3,pc}$ as mentioned
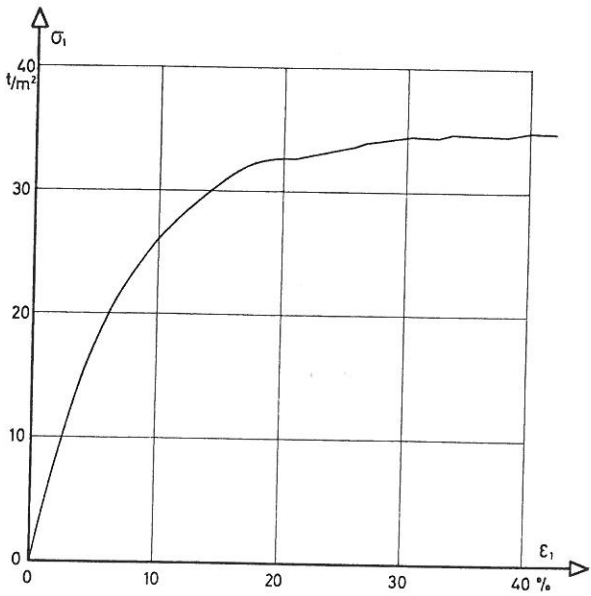
Fig. 2.15 A performance curve for an undrained compression test, showing that no peak point or weakening of the sample occurs even at large deformations. Kratbjerg moraine clay.

above. After that follows an isotropic unloading until the actual magnitude of $\bar{\sigma}_3$ before the first failure stage. Between each stage this procedure is repeated to ensure the same state of the sample before testing.

The test results can be given in a stress path $\frac{1}{2}(\sigma_1 + \sigma_3)$ versus $\frac{1}{2}(\sigma_1 - \sigma_3)$. A preconsolidated clay tries to expand under great shear stresses and this is prevented by increasing the cell pressure. This causes the failure shear stress to increase until the so-called critical state where vertical deformations take place without volume change at constant stresses. In fig. 2.17 it can be seen that for great shear stresses this stress path has a straight asymptote, and by comparing with similar curves from different stages it can be seen that these curves actually have nearly the same asymptote. This line is therefore assumed to represent the failure state just as the Mohr envelopes does, but it is possible to find this line in a single test and in this way to determine both the undrained shear strength and the effective strength parameters
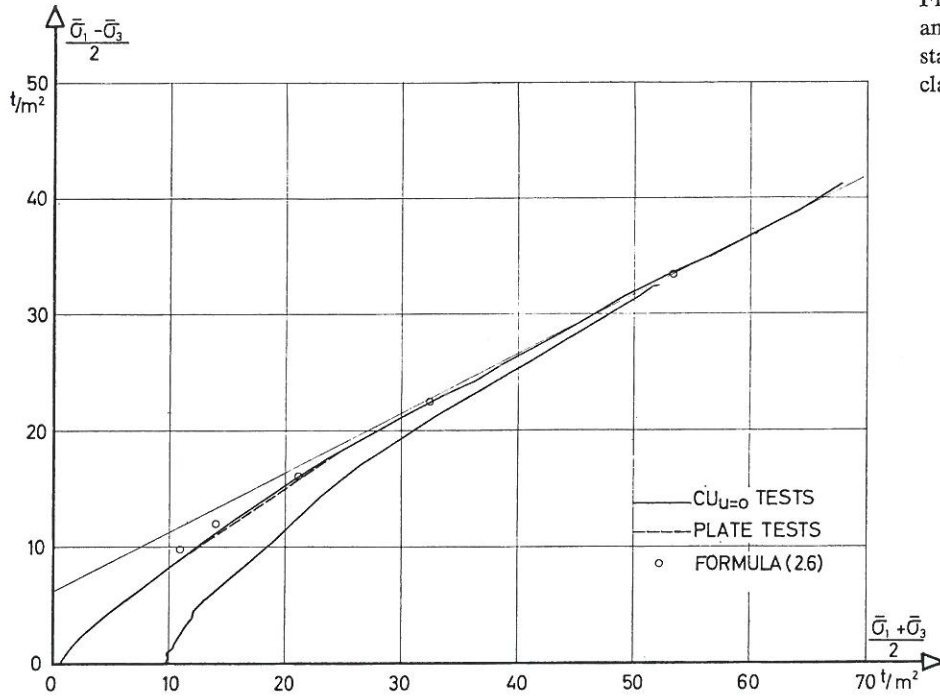
Fig. 2.16 A multiple stages test.
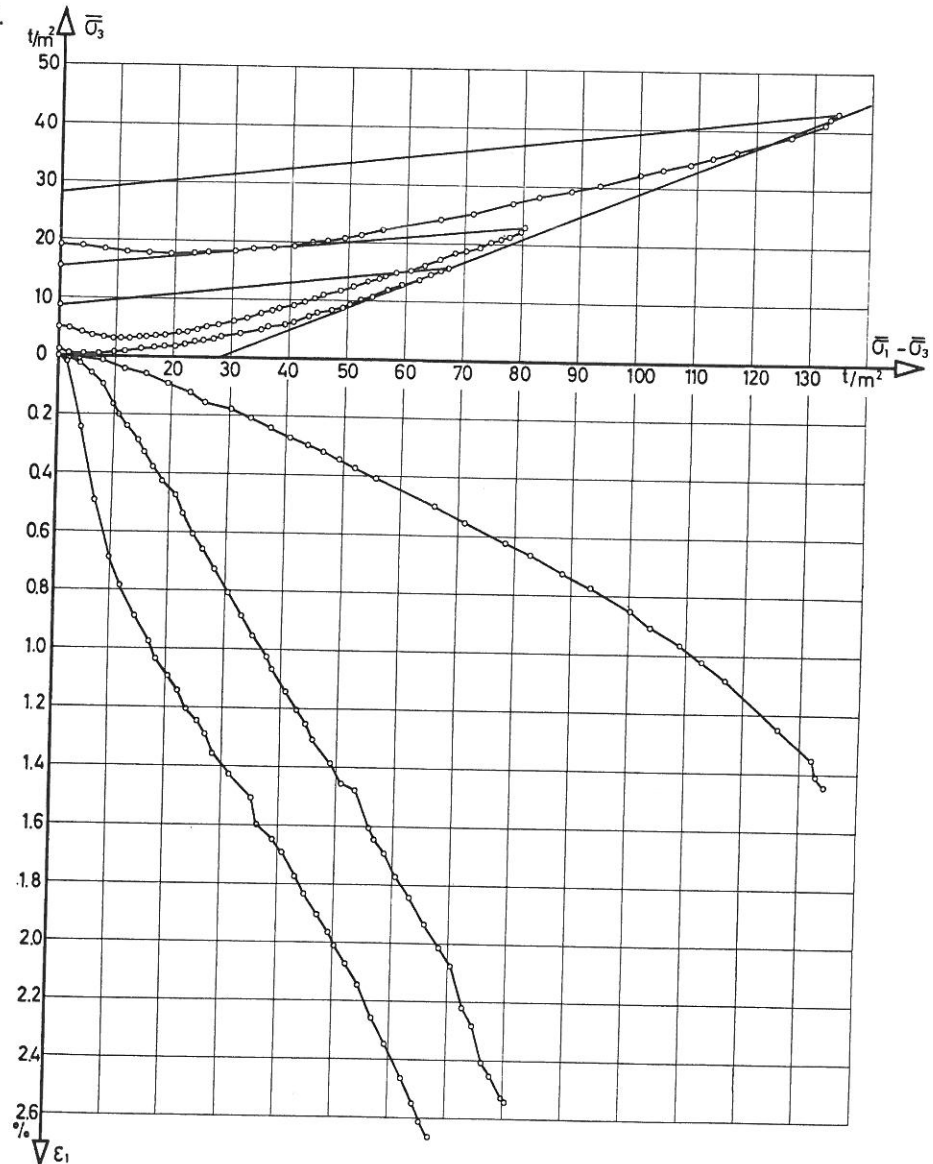
Fig. 2.17 Effective stress-path in an undrained triaxial multiple stage test on Carlsberg moraine clay, heavily preconsolidated.

(strictly speaking the real ones). For normally consolidated clays it is not possible to determine the effective (or real) strength parameters in a single-stage test.

Multiple-stage tests give the stress path curve for relatively small deformations ($\varepsilon_1 < 2\,\%$), but the undrained shear strength deformation normally requires more than 10 % vertical deformation. It would there-

TABLE 2.5

Effective strength properties measured in triaxial tests

Locality	Tests with fixed ends $H = 2D$, $A = 10\ cm^2$		Tests with free ends $H = D$, $A = 38.5\ cm^2$	
Sabro	$\overline{\varphi} = 26°4$	$\overline{c} = 1.4\ t/m^2$	$\overline{\varphi} = 29°6$	$\overline{c} = 1.27\ t/m^2$
	$= 30°0$	$= 0\quad -$	$= 32°0$	$= 0.90\quad -$
	$= 28°0$	$= 1.0\quad -$		
	$\overline{\varphi}_m = 29°8$	$\overline{c}_m = 1.15\ t/m^2$	$\overline{\varphi}_m = 30°6$	$\overline{c}_m = 1.1\ t/m^2$
Odense I			$\overline{\varphi} = 34°2$	$\overline{c} = \ ?\ t/m^2$
			$= 34°5$	$= 2.9\quad -$
			$= 35°0$	$= 1.3\quad -$
			$\overline{\varphi}_m = 34°5$	$\overline{c}_m = 2.9\ t/m^2$
Kratbjerg	$\overline{\varphi} = 33°7$	$\overline{c} = 2.35\ t/m^2$	$\overline{\varphi} = 30°8$	$\overline{c} = 3.95\ t/m^2$
	$= 34°5$	$= 0\quad -$	$= 34°2$	$= 3.45\quad -$
	$= 30°0$	$= 3.90\quad -$	$= 30°8$	$= 4.25\quad -$
	$\overline{\varphi}_m = 32°0$	$\overline{c}_m = 3.05\ t/m^2$	$\overline{\varphi}_m = 32°6$	$\overline{c}_m = 4.0\ t/m^2$
Carlsberg II	$\overline{\varphi} = 26°4$	$\overline{c} = 2.2\ t/m^2$		
	$= 32°5$	$= 2.35\quad -$		
	$= 28°4$	$= 3.42\quad -$		
	$\overline{\varphi}_m = 30°6$	$\overline{c}_m = 2.84\ t/m^2$		
Carlsberg I	$\overline{\varphi} = 32°0$	$\overline{c} = 2.8\ t/m^2$	$\overline{\varphi} = 31°0$	$\overline{c} = 7.1\ t/m^2$
			$= 34°0$	$= 7.2\ t/m^2$
			$\overline{\varphi}_m = 33°0$	$\overline{c}_m = 7.2\ t/m^2$

fore be useful to have a formula for undrained performance curves in order to determine undrained shear strength from multiple-stage tests.

In table 2.5 the results of 20 $CU_{u=0}$ tests are shown. 10 of these tests were made in the normal apparatus with height of sample equal to twice the diameter. $\bar{\varphi}_m$ and $\bar{c}_m$ are the strength parameters for a Mohr envelope, including all the tests under consideration. Fig. 2.18 shows that the effective angle of internal friction is almost constant (the variation is 2° for e varying from 0.50 to 0.25) and that the cohesion varies with the void ratio:

$$\bar{c} = 43 \; \exp(-7.3 \cdot e_k)$$
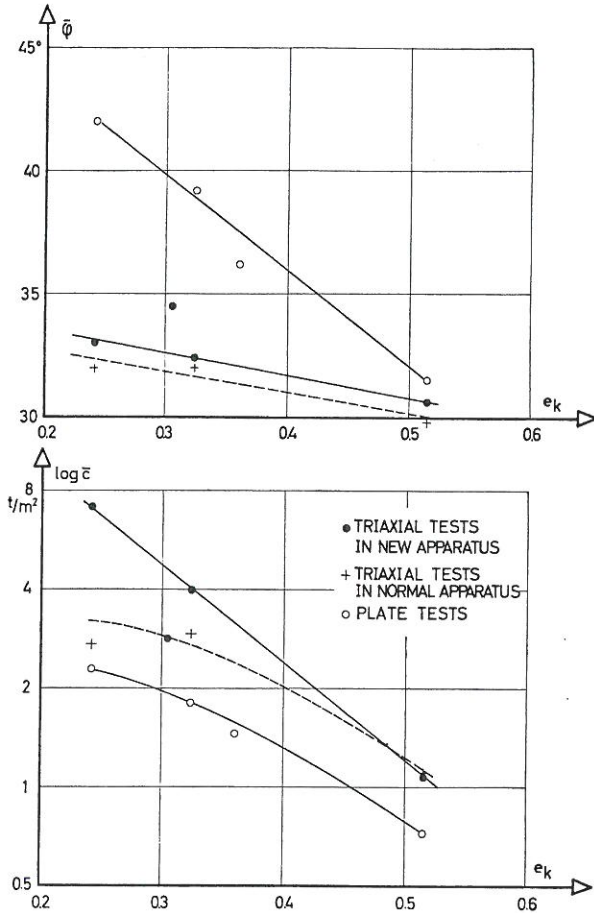
as presumed by Hvorslev.

Fig. 2.18 Results from laboratory tests with free and fixed ends compared with results from plate tests.

These results were checked by a series of *CD*-tests on Kratbjerg moraine clay. The *CD*-test consists of two parts. First, an isotropic and drained reconstruction of the stress history, and an isotropic unloading until the actual pressure. In the second part a drained test with constant cell pressure is carried out with a very low rate of strain. Multiple-stage tests cannot be performed, which means that one sample can only give one failure value. This kind of test is therefore very expensive and time-consuming. It can be seen in fig. 2.19 that these tests give the same strength parameters as mentioned above.
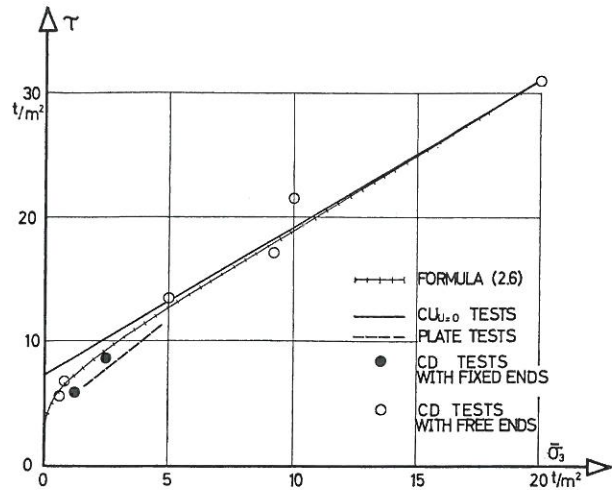

Fig. 2.19 Results from drained triaxial tests with constant cell pressure compared with results from undrained multiple stage test and drained plate tests. Kratbjerg moraine clay.

The influence of stress level

The results of laboratory tests show that for higher stress levels ($\sigma_3 > 10$ t/m²) the effective strength parameters $\bar{c}$ and $\bar{\varphi}$ describe the failure state very well. For lower values of $\bar{\sigma}_3$, fig. 2.19 also shows that the failure curve bends away from the line towards the origo, giving greater values of the friction angle and smaller values of the cohesion.

The strength proporties used in this paper are always the "tangent" friction angle φ_t and the corresponding cohesion c_t. Another set of strength proporties is the "secant" friction angle φ_s with the corresponding cohesion c_s being zero.

Coulomb's failure condition is:

$$\frac{\bar{\sigma}_1 - \bar{\sigma}_3}{2} = \frac{\bar{\sigma}_1 + \bar{\sigma}_3}{2} \sin \bar{\varphi}_t + \bar{c}_t \cos \bar{\varphi}_t$$

or

$$\tau = \frac{\sin \bar{\varphi}_t}{1 - \sin \bar{\varphi}_t} \bar{\sigma}_3 + \frac{\bar{c}_t \cos \bar{\varphi}_t}{1 - \sin \bar{\varphi}_t} \qquad (2.5)$$

where

$$\tau = \tau_{max} = \frac{1}{2}(\bar{\sigma}_1 - \bar{\sigma}_3)$$

A formula including the influence of the stress level can be evaluated from 2.5.

$$\tau = \frac{\sin \bar{\varphi}_a}{1 - \sin \bar{\varphi}_a} \bar{\sigma}_3^n (\bar{\sigma}_3 + \sigma_o)^{1-n} \qquad (2.6)$$

where $\sigma_o = \dfrac{\bar{c}_a}{1-n} \cot \bar{\varphi}_a$ and the suffix a denotes asymptotical parameters.

These expressions coincide for $n = 0$ or $\bar{c} = 0$, and for other values of n, the curved envelope of effective failure condition 2.6 has the usual failure condition 2.5 as an asymptote.

Fig. 2.19 shows some results of drained triaxial

tests with constant cell pressure. The curve representing formula 2.6 determines a value of $n = 0.2$. Since the line 2.5 is asymptote to 2.6, this line always gives bigger values of τ than 2.6 does. In order to obtain a closer agreement the value of $\bar{c}_a$ in 2.6 is chosen 5 % higher than that in 2.5.

n probably depends on the void ratio but can here only be determined in one case, so we have to take n as a constant until further information is available.

The four points shown in fig. 2.17 serve as a control of 2.6.

Comparison of field and laboratory results

Before a comparison between test results obtained in the field and in the laboratory is made, some effects should be pointed out which makes the comparison difficult. These are the influence of stress level, differences between plane and triaxial failure conditions and the influence of progressive rupture.

Triaxial tests are usually carried out at a *stress level* greater than 5 t/m² at the beginning of the test.

In plate tests the surface load varies from 0.5 — 3 t/m².

According to Meyerhof (1950) the characteristic stress level for plate tests on sand corresponds to about 10 % of the failure load. However, a difference between sand and clay motivates another characteristic stress level for clay.

For sand the void ratio is mostly dependent on how the sand has been deposited and only to a smaller extent on the stress level, so that the structure of sand layer is preserved even for a totally unloaded sand.

However, moraine clay expands at small stress levels. This expansion is nearly proportional to the logarithm of the overconsolidation ratio, $\log(\bar{\sigma}_{pc}/\bar{\sigma})$. In the totally unloaded state the liquid limit is exceeded, as can be observed when a moraine clay surface is flooded. This liquid layer is very thin, only 2–3 mm, but the swelling effect is obvious in the upper 15–20 cm as may be concluded from fig. 2.11, where the stress level is at least 0.35 t/m². The swelling alters the soil properties of a heavily preconsolidated moraine clay so much that it might be more correct to assume that the effective overburden pressure in the middle of the rupture zone represents the stress level. This stress level is for $\bar{\varphi} = 30°$ only half as great as Meyerhof's characteristic stress level.

For plate tests the effective surface load represents the stress level, except for very small stress levels where even the extension of the rupture figure is important.

This assumption agrees with the fact that the tests in which swelling was allowed showed bearing capacities less than expected from tests at higher stress levels (fig. 2.11).

A difference in *plane and triaxial failure conditions* influences the test results. In circular plate tests the plane angle of friction is determined, because the shape factors are a result of comparing tests on very long plates and on circular plates.

The plane parameters should theoretically be somewhat greater than the triaxial ones and therefore this effect should give larger failure loads for plates than calculated on the basis of triaxial tests.

In the most faultless laboratory tests failure exists as a uniform plastic zone throughout the sample. This means that all parts of the sample are at failure at the same time and the performance curve represents every element of the sample.

Rupture under a circular plate or foundation is much more complicated and consists of plastic zones and rigid bodies. Some parts of the soil will dilate. The stress and strain distribution is not uniform and rupture first takes place in some parts of the soil. In a soil which dilates under failure conditions these regions weaken and the *rupture will be progressive,* giving smaller failure loads than those calculated on the basis of triaxial tests.

Undrained tests

Undrained plate tests and vane tests were carried out under constant circumstances and unconfined compression tests were performed on samples subjected to nearly the same stress level.

It has already been mentioned that when the volume is kept constant no weakening of the soil occurs, even at very large deformations. Therefore the rupture cannot be progressive.

Differences between results of undrained plate tests and laboratory tests if any, would then mainly be due to differences in plane and triaxial failure conditions.

As already mentioned no differences are actually observed, and the influence of plane versus triaxial failure conditions may thus be of minor importance.

Drained tests

The results of drained plate tests and drained triaxial tests are shown in fig. 2.18.

In drained triaxial tests the samples expand under great shear stresses and get weaker. On the performance curve the effect of expansion is seen as a peak point (fig. 2.20).

In plate tests the soil also expands and after failure the void ratio varies all over the rupture zone. Since the friction angle $\bar{\varphi}_a$ (represented by the black points) only varies a little with the void ratio, compared with the cohesion $\bar{c}_a$ (represented by the black points too), it seems to be an appropriate assumption that $\bar{\varphi}_a$ is constant all over the rupture zone, but that $\bar{c}_a$ varies, due to the influence of progressive rupture.

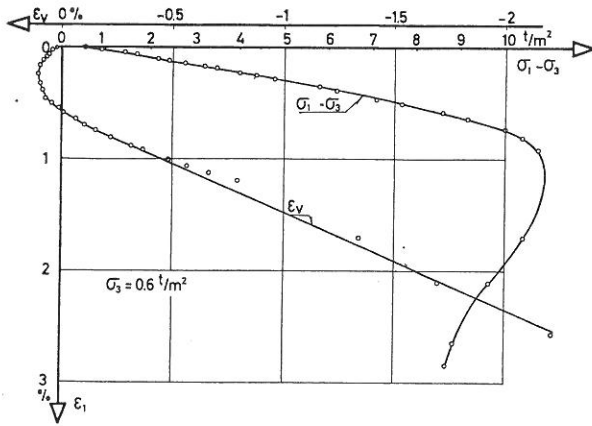The effects of the stress level and a difference be-

Fig. 2.20 A performance curve for a CD test.

Comparison of laboratory tests and plate tests

	Kratbjerg	Carlsberg	Sabro
e	0.324	0.242	0.515
q_m t/m²	$\sim$ 1.2	$\sim$ 2.3	$\sim$ 0.5
$\overline{\varphi}_{tr}, \overline{\varphi}_p$	38°4	42°0	31°5
c_{tr} t/m²	2.6	4.0	1.0
c_p t/m²	1.84	2.3	0.75
$\overline{\sigma}_{3,c}$ t/m²	2.4	1.8	2.2
Meyerhofs stress level, t/m²	$\sim$ 20	$\sim$ 50	$\sim$ 4

tween plane and triaxial failure conditions causes $\overline{\varphi}_p > \overline{\varphi}_a$, where p denotes plate tests. Fig. 2.18 shows that the difference between $\overline{\varphi}_a$ and $\overline{\varphi}_p$ decreases for increasing e_k and that for a certain value of $e_k > 0.52$, $\overline{\varphi}_a = \overline{\varphi}_p$. For this value of e_k the effects of stress level and plane and triaxial failure conditions do not occur. Since the difference between plane and triaxial failure conditions is normally assumed to depend on the amount of $\overline{\varphi}_a$ only, this indicates that the difference between plane and triaxial failure conditions can be neglected, and that differences between $\overline{\varphi}_a$ and $\overline{\varphi}_p$ are mainly due to variations in the stress level.

By use of formula 2.6 it is possible to show that this assumption leads to reasonable results. By differentiation we get:

$$\frac{\sin \overline{\varphi}_t}{1 - \sin \overline{\varphi}_t} = \frac{\sin \overline{\varphi}_a}{1 - \sin \overline{\varphi}_a} \left(\frac{\overline{\sigma}_3}{\overline{\sigma}_3 + \sigma_o} \right)^n \left(1 + n \frac{\sigma_o}{\overline{\sigma}_3} \right)$$

and

$$\overline{c}_t \cot \overline{\varphi}_t = \frac{(1 - n) \sigma_o \overline{\sigma}_3}{\overline{\sigma}_3 + n \sigma_o}$$

The plate tests on Kratbjerg moraine gave $\overline{\varphi}_p = 38°4$ and a mean value of the cohesion $\overline{c}_p = 1.84$ t/m². In triaxial tests $\overline{\varphi}_t = 38°4$ at $\overline{\sigma}_3 = 2.4$ t/m² and here $\overline{c}_t = 2.6$ t/m². The effect of progressive rupture can be seen by the reduction of $\overline{c}_t$ from 2.6 to 1.8 t/m². Table 2.6 shows similar results for a heavily preconsolidated clay (Carlsberg I) and a slightly preconsolidated clay (Sabro).

The characteristic stress level $\overline{\sigma}_{3,c}$ is also given in table 2.6. For a slightly preconsolidated moraine clay (Sabro), Meyerhof's assumption gives nearly the same stress level as here calculated, but in the two other cases the effective overburden pressure in the middle of the rupture figure is a better approximation.

Conclusion

Plate tests and laboratory tests have been carried out on different Danish moraine clays, but the results show that they can all be treated as one clay, although with different void ratios. The strength properties are shown in figs. 2.6 and 2.18, being valid for stress levels higher than 5 t/m². The effective cohesion $\overline{c}$ can be expressed as follows:

$$\overline{c} = 43 \exp (- 7.3 \, e_k)$$

and also $\overline{\varphi}$ varies a little with the void ratio:

$$\overline{\varphi} = 35°3 - 9° \, e_k \quad (0.25 < e_k < 0.5)$$

The undrained shear strength can be expressed by:

$$c_u = \exp (0.77 + e_k^{-1.2})$$

By use of the formula for bearing capacity 2.3 with the shape factors $s_c^o = s_c = s_q = 1.2$ it is possible to calculate strength parameters from plate tests.

The difference between these results and those obtained in the laboratory can mostly be explained by differences in stress levels, and the progressive rupture in drained plate tests also seems to have some influence. Differences in plane and triaxial failure conditions are of minor importance, as well in the drained state as in the undrained state.

The strength properties of moraine clay vary in such a way that the long-term bearing capacity is greater than the short-term bearing capacity for all foundations occurring in practice. Consolidation is normally finished already during the construction period, because the coefficient of permeability is at least 100 times bigger for moraine clay than for normal clays. This means that the long-term bearing capacity is relevant and that therefore the factor of total safety is normally greater than 1.75, which corresponds to the short-term bearing capacity calculated from vane tests as specified in the Danish Code of Practice for Foundation Engineering.

Oedometer tests

The calculation of settlements is usually based on oedometer tests, because the standard apparatus is relatively inexpensive, and the experience often shows results in agreement with the observed settlement, as mentioned in the next chapter.

For firm soils it is necessary to use "inelastic" apparatus, however. Such an apparatus is described in detail in Paper 1, and here the testing method and the different factors influencing the results are mentioned too. These factors are the preconsolidation of the sample, the preparation of the sample, the adaptation of the sample to the ring, remoulding and ageing effects. The influence of these factors can be minimized by using the following test procedure.

First the sample gets a preloading until $\bar{\sigma}_{max}$, which approaches the natural preconsolidation pressure $\bar{\sigma}_{pc}$ as nearly as possible. After unloading until $\bar{\sigma}_u$ and reloading until $\bar{\sigma}_{max}$ new un- and reloading cycles follow new values of $\bar{\sigma}_u$ but to the same $\bar{\sigma}_{max}$. Normally $\bar{\sigma}_u$ gets smaller during the test in order to avoid irreversibilities due to secondary compression at the highest pressure.

Tests performed with increasing $\bar{\sigma}_u$ indicate that this is the only difference between these two test procedures. The vertical load increases from two to three times per step in reloading, and from two to ten times in unloading.

Each test consists of 35–95 loading steps and the reloading and unloading curves from 42 tests on 8 different moraine clays should here be statistically treated.

The state of stresses

In a standard oedometer it is normally impossible to measure the stresses between the ring and the sample σ_h, but a triaxial apparatus can give reasonable results, if filter effects and membrane misfits are minimized (Paper 1). Since no friction occurs in the triaxial test, the deformations measured here should be somewhat greater than those measured in oedometer tests.

Several loading procedures were examined and it was found that the best method is to follow the loading procedure in an oedometer test as closely as possible. At the time $t = 0$ an isotropic stress increment is applied, corresponding to fully saturated oedometer samples. During each loading step the cell pressure is decreased synchronously with an increasing vertical deviator pressure in such a way that the total vertical pressure is constant and no horizontal deformations occur. In this way it is even possible to obtain reasonable time curves (Fig. 2.21).
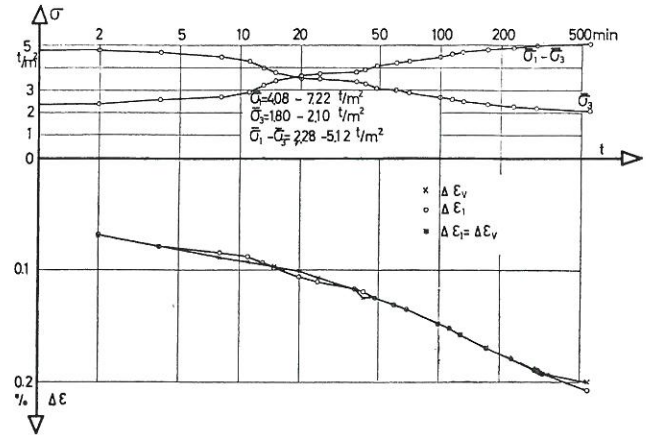

Fig. 2.21 A time curve from a triaxial test with constant area, showing volumetric and vertical strains and effective vertical and horizontal stresses.
Sabro moraine clay.

Reloading from an initial isotropic state can easily be carried out, but unfortunately it is only possible to follow the unloadings to an isotropic state. If the vertical pressure gets smaller than the horizontal one, the creation of a distinct rupture surface prevents uniformly distributed deformations, even influencing the test results for small deviator stresses.

The coefficient of earth pressure at rest $K_o = \bar{\sigma}_h/\bar{\sigma}_v$ varies very much during unloading and reloading (fig. 2.22), but in reloading K_o reaches a final value K_o^f in the last part of the recompression. During unloading K_o increases and when the consolidation ratio $r_c = \bar{\sigma}_v/\bar{\sigma}_{v,\,max}$ is ~ 0.1 an isotropic state occurs. When the unloading continues the horizontal stresses become bigger than the vertical ones.
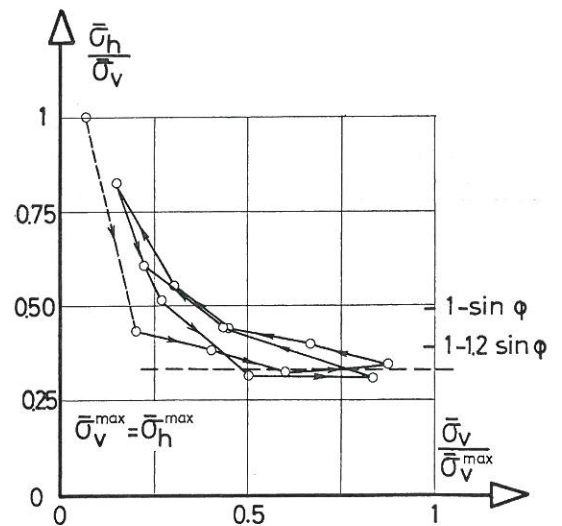

Fig. 2.22 The variation of the coefficient of earth pressure at rest during unloading and reloading. Sabro moraine clay.

These results conform to investigation made by Brooke and Ireland in Hendron's oedometer, which has a thin ring with corrective motion. On the unloading of sand the isotropic state takes place for $r_c = 0.1$ to 0.2, and K_o approaches the coefficient of passive earth pressure for small values of σ_u. For clay $r_c = 0.20$ to 0.25 seems to give an isotropic state.

In primary loading for clays K_o measured in the same apparatus is found to be

$$K_o = 1 - 1.2 \sin \overline{\varphi}$$

whereas for sand

$$K_o = 1 - \sin \overline{\varphi}$$

These values of K_o are seen to be somewhat larger than the K_o^f measured here.

An empirical formula

Brinch Hansen has proposed the following formulas for recompression tests:

$$\varepsilon_{rb} = -a \log \left[\frac{a\overline{\sigma} + \overline{\sigma}_{max} + b}{(a + 1)\,\overline{\sigma} + b} \right] \qquad (2.7a)$$

$$\varepsilon_{rc} = a \log \left[\frac{a\overline{\sigma}_u + \overline{\sigma} + b}{(a + 1)\,\overline{\sigma}_u + b} \right] \qquad (2.7b)$$

where $\overline{\sigma}$ is the effective vertical pressure. These formulas fulfil the condition of reversibility, i.e. ε_{rb} for $\overline{\sigma} = \overline{\sigma}_u$ is equal to ε_{rc} for $\overline{\sigma} = \overline{\sigma}_{max}$.

These formulas are used in a statistical treatment of oedometer tests.

Statistical treatment

Some of the constants in formula 2.7 may depend on the void ratio, and if we want to express the remoulding effect occurring beyond the preconsolidation pressure, a power function of $\overline{\sigma}_{max}/\overline{\sigma}_{pc}$ should be involved in a. But here only tests with $\overline{\sigma}_{max} \sim \overline{\sigma}_{pc}$ will be treated.

The best estimate of the constants α, a and b is found from test results by adjustment by elements. The ε-values of each recompression curve are corrected for the friction developed by unloading. These corrections are also treated as elements, making the number of them very large (e.g. recompression on Kratbjerg has 42 elements). This friction results in too small deformations, especially for small stress increments. The generation of friction during unloading changes these curves considerably.

Since these formulas should be used for settlement analysis, the recompression and rebound curves will be treated separately in order to stop this systematical error in the rebound curves from influencing the constants in the recompression curves.
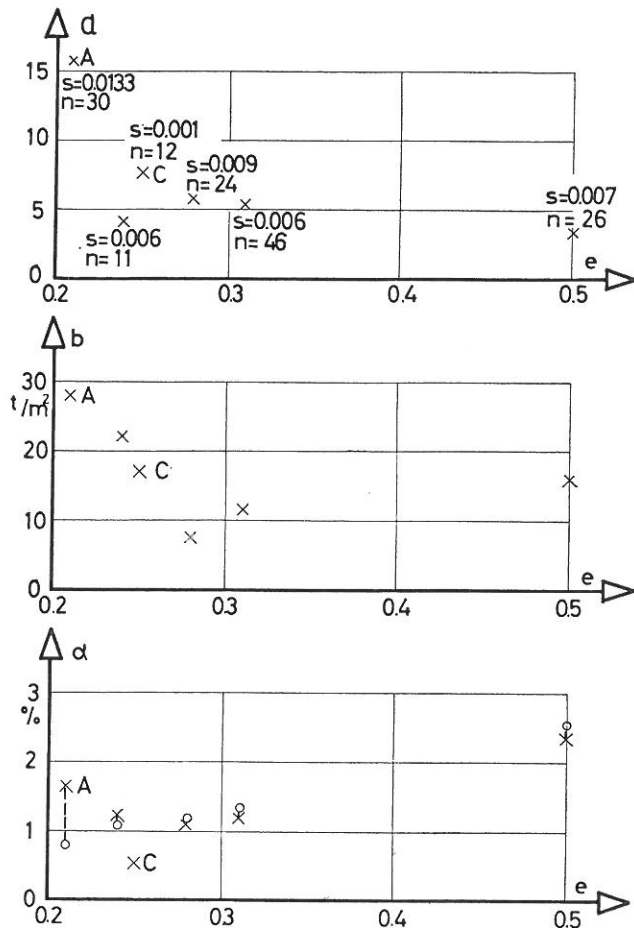

Fig. 2.23 The constants in formula (2.7) determined by treating each soil separately. The circles mark the new values of α when regarding a and b as constants.

First each kind of moraine clay is treated separately, whereby the void ratio is nearly constant. The elements determined by this method are given in fig. 2.23 where the number of elements n and the standard deviation on ε_{rc} can be seen too. The points marked C represent a moraine clay with 58 % Calcite and correspond to relatively smaller deformations than the other points.

If we first neglect Point A, a and b can be taken as constants and the variation with e can for simplicity be assumed to occur in α only. It can be shown that a, b and α are correlated in such a way that if these three quantities are changed proportionally the standard deviation does not change considerably. Point A can be moved from the cross points to the transparent points with a change in standard deviation from 0.133 % to 0.165 % only. Therefore the moraine clays including A but not C will be treated as one clay with varying void ratio.

$$\varepsilon_{rc} = a' \frac{e^m}{1 + e} \log \left[\frac{a\overline{\sigma}_u + \overline{\sigma} + b}{(a + 1)\,\overline{\sigma}_u + b} \right] \qquad (2.7c)$$

Using this formula the standard deviation becomes of course somewhat larger. An adjustment by ele-

37

ments ($n = 126$) gives $\alpha = 0.115$, $m = 1.5$, $a = 5.0$ and $b = 1.7$ t/m². The standard deviation on ε_{rc} is 0.10 %.

Some of the tests are shown in fig. 2.24 together with curves corresponding to elements, which give the best approximation to the clay in question and not only to the tests shown here.

The use of formula (2.7c) including the void ratio gives reasonable results even for the Carlsberg moraine clay marked A in fig. 2.23. This can be seen in fig. 2.25.

It has already been mentioned that friction between the pistons and the oedometer ring increases during unloading. By means of formula 2.7 the rebound curves can be determined from the reloading curves. In fig. 2.26 and 2.27 these curves are compared with test results and give a friction of the same order of magnitude as the vertical stress itself. This agrees well with the normal shape of recompression curves.

In triaxial tests no friction occurs. In fig. 2.27 the results of an unloading with constant area are compared with the theoretical curve (formula 2.7).

This shows that formula 2.7 approximates the test results very well. The parameters are determined from reloading curves only and thus the formula can be used in the conventional settlement analysis.
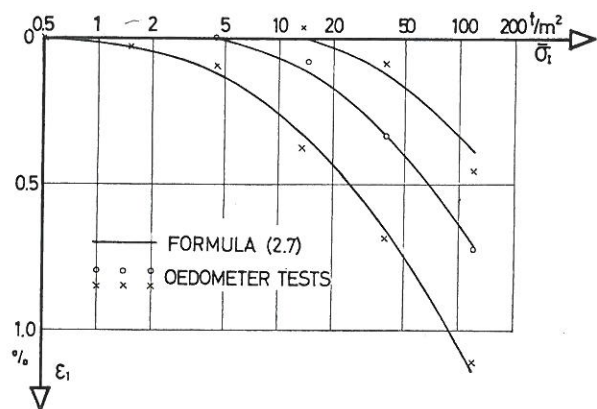

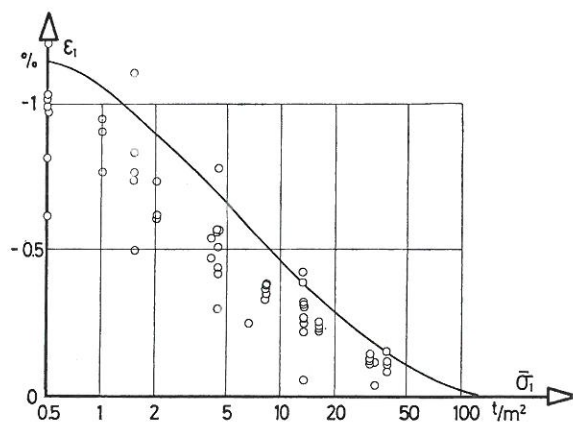Fig. 2.24 Reloading curves with the best estimates of the constants.

Fig. 2.26 Rebound curves compared with formula 2.7 showing a reasonable amount of the friction in unloading. Kratbjerg moraine clay.
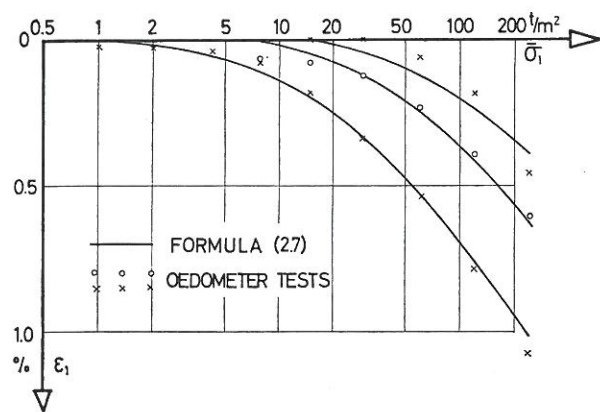

Fig. 2.25 Reloading curves with constants covering different values of the void ratio. Carlsberg moraine clay marked A in fig. 2.23.
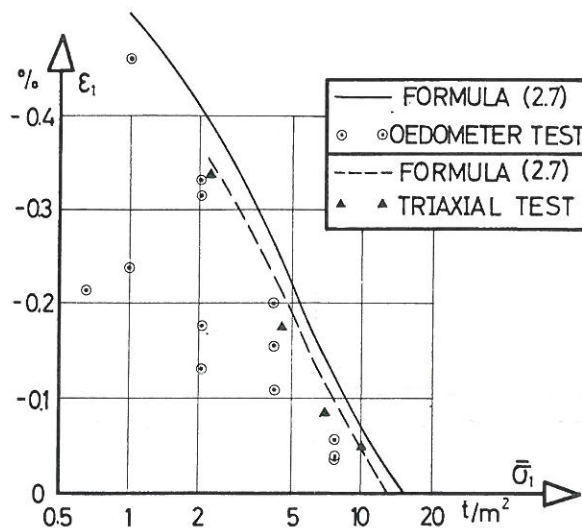

Fig. 2.27 Rebound curves on Sabro moraine clay.

38

Isotropic compression tests

Some isotropic compression tests have been carried out, following the same test procedure as used in the oedometer tests. 23 loading cycles performed on three different moraine clays can be treated statistically in the same way as described previously on the basis of formula (2.7c).

These test results are not influenced by friction, which is the gravest source of error when making oedometer tests. The variation of the temperature and membrane misfits cause some errors and complicate the determination of the drained state, but these are minimized as described in Paper 1. Therefore the standard deviation is in these tests smaller than that determined in oedometer tests. In the following ε denotes the vertical deformation.

An adjustment by elements gives $\alpha = 0.92$ %, $a = 1.6$, $b = -0.006$ t/m² and $m = 0.433$. The standard deviation on ε_{rc} is 0.021 % only, much smaller than determined in oedometer tests. Formula (2.7c) assumes ε_{rc} to be dependent on e, but it can be shown that $m = 0.43$ corresponds to a minimum influence of e and this indicates that ε_{rc} may be almost independent on e. Using formula (2.7b) we get nearly the same standard deviation ($s = 0.021$ %) showing that ε_{rc} is independent on e.

Equation (2.7c) can now be reduced to

$$\varepsilon_{rc} = 0.4 \log \left[\frac{1.6\ \sigma_u + \sigma}{2.6\ \sigma_u} \right] \% \qquad (2.8a)$$

One of these tests with four reloading cycles is shown in fig. 2.28 together with curves calculated by means of (2.8a).
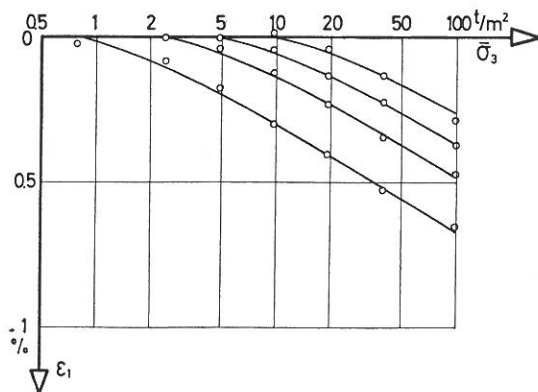

Fig. 2.28 Isotropic reloading curves.

The corresponding formula for rebound is

$$\varepsilon_{rb} = - 0.4 \log \left[\frac{1.6\ \sigma_u + \sigma_{max}}{2.6\ \sigma_u} \right] \% \qquad (2.8b)$$

and shows that ε_{rb} becomes infinite in the totally unloaded state. This corresponds with observations of clay surface flooded by water. A thin superficial layer swells until the water content has exceeded the liquid limit.

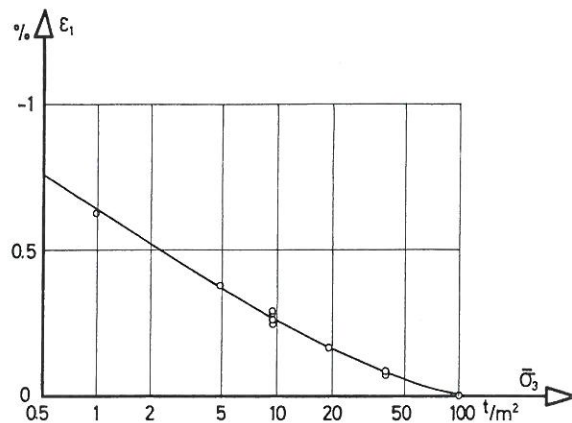In fig. 2.29 a rebound curve, calculated on the basis of (2.8 b), is compared with test results.

Fig. 2.29 Isotropic rebound curve.

In oedometer tests b is three times larger than a and indicates a final value of ε_{rb}. But in these tests the stress paths are very complicated (fig. 2.22) and distorsion occurs for small stresses in reloading curves. This changes the b-value very much compared with the isotropic compression tests. ε_{rb} has a final value in oedometer tests because it is impossible to unload the sample totally because of friction between sample and oedometer ring but of course the formulas (2.7) should not include any deficiencies in the apparatus. However, this difference between the formula and the theory is not appreciable except for loadings smaller than normally used, as already shown.

Therefore the same formula system can be used as well for isotropic compression tests as for oedometer tests.

Settlement analysis

In this paper the previously mentioned deformations measured in laboratory tests will be checked by means of plate tests and settlement observations of structures.

When comparing laboratory results and field results settlement calculations are necessary, and therefore we first have to describe the theoretical basis of these calculations, here especially for the centreline beneath

circular footings. The stress distribution is in this case axi-symmetrical as in the laboratory tests.

The plate tests were carried out on different moraine clays. Here 36 drained tests on Kratbjerg moraine clay ($e = 0.32$), 5 drained tests on Carlsberg and Rigshospitalets moraine clay ($e = 0.24$) and 2 tests on Sabro moraine clay ($e = 0.52$) will be mentioned. The test procedure is described in the second chapter.

Three settlement observations were performed on structures built on moraine clay, which was tested in the new apparatus. These are the grain silos of "Carlsberg" in Copenhagen, and of "Muus" in the harbour of Odense, and an ammonia silo of "Ammonia" in Odense. The last mentioned was extremely carefully observed, including measurements of the deformations of the upper 7.5 m layer and of the upper 2.4 m layer.

Theoretical Methods

The application of a vertical load to a horizontal area of the surface of a soil stratum produces stresses within the soil mass and causes deformations in the soil and sinking of the structure.

It is difficult to find a solution which is both statically and kinematically correct. There exists namely as yet no formula for deformations taking into account rotation of the principal directions of stresses. We therefore have to use a semi-empirical method, which consists of two phases. First the stress distribution in the centreline beneath the foundation is determined approximately, and the corresponding deformations can then be computed by means of deformation formulas for axi-symmetrical loading.

The stresses can be calculated by means of statical solutions with fulfilled equilibrium conditions and without failure in any part of the soil mass. The last requirement can often not be fulfilled, however.

Such a method is based on Boussinesq's equations for the stress distribution in a semi-infinite, isotropic, homogeneous and elastic solid caused by a vertical point load on the horizontal surface of the solid. These equations show that the vertical stresses in the centreline are independent of the elastic properties of the material, whereas the horizontal stresses depend on Poisson's ratio μ.

Another method is proposed by Frölich, who assumed the maximum normal stress to be directed towards the point of loading. In the undrained case ($\mu = \frac{1}{2}$) this solution coincides with the theory of elasticity, but for $\mu < \frac{1}{2}$ the theoretical properties of the solid better approximate those of the soil, (increasing stiffness with depth). By this method the stresses become bigger than those calculated by the previous method. When comparing the settlements on moraine clay computed by the two methods we find a difference of only about 10 percent.

In this paper Boussinesq's formulas will be used, and the theoretical settlements will then probably be too small.

Some other problems have been solved by use of the theory of elasticity. Burmeister (1956) has treated a two layer soil system in which the underlying layer is rigid. Such a rigid layer causes concentrations in the stress distribution in the surface layer and makes the deformations of this larger. For moraine clay with increasing stiffness with depth this seems to be of minor importance. An example shows an increase of settlement of about 3 percent.

Kezdi has elaborated formulas for a point load acting below the surface of the solid. The stresses beneath the point load are smaller than usual because some of the load is taken by the overlaying solid. It is assumed that the load is surrounded by elastic material. But when the footing is placed at a certain depth below the surface, some of the soil is of course excavated, and the theoretical case does not apply. However, if the sides of the foundation are cast against the sides of the excavation or if the excavation is filled up with a material stiffer than the soil proper, the sides of the excavation are prevented from moving and the settlement becomes smaller. Some of the load can be carried by friction forces along the side. Sometimes this effect is approximated by the theory of Kezdi, but usually the fill is softer than moraine clay and therefore this theory is seldom useful.

When loading the surface of the soil in an area of arbitrary shape, the stress distribution can be calculated by integration of the basic equations.

If the load is applied through a rigid foundation a deformation condition at the surface gives the distribution of the contact pressure. A rigid circular foundation has the well-known distribution

$$p_r/p = \frac{1}{2} (1 - r/r_o)^{-\frac{1}{2}}$$

If the stiffness of the soil increases with depth, even the use of the theory of elasticity gives a contact pressure distribution which is more concentrated in the middle of the foundation, and that causes greater stresses in the centreline beneath the foundation. The increase of stresses is a function of the depth z and the relative modulus increment α defined by:

$$K_z = K_{fl} (1 + \alpha z/D) \qquad (2.9)$$

where K_{fl} denotes the consolidation modulus in the foundation level and D is the diameter of the plate. This function is calculated numerically for circular foundations (EDP) and the result is seen in fig. 2.30.
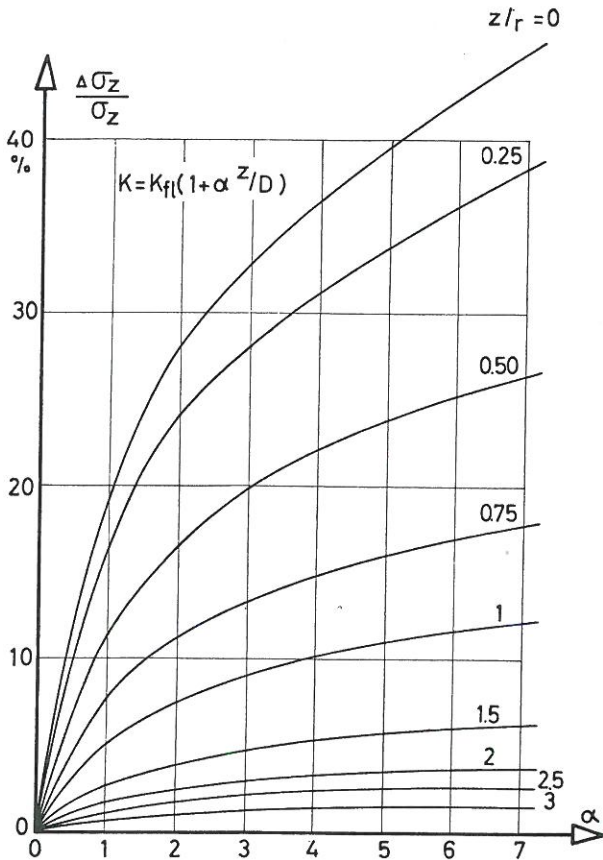
Fig. 2.30 Increasing stiffness with depth causes concentrations of the stresses in the centreline beneath a foundation.

First σ_z is determined by means of Boussinesq's formulas and the curves give the relative additional concentration in the centreline.

If the footings are of great length the stress condition is nearly plane. In this case the stress distribution is different from the previously mentioned distribution and of course this should be taken into account when calculating the settlements, but these are furthermore influenced by the intermediate principal stress. The vertical deformation can be expressed as

$$\varepsilon_1 = \frac{1+\mu}{E} [(1-\mu)\, \sigma_1 - \mu\sigma_3]$$

In the undrained case $\mu = \frac{1}{2}$ and

$$\varepsilon_1 = \frac{3}{4} \frac{\sigma_1 - \sigma_3}{E}$$

Since the undrained settlements in moraine clay comprise about 80 percent of the total settlements, it seems reasonable to use this factor in the drained case too. Therefore we must first determine the stress distribution and calculate a settlement d_s and then make a correction to get the right value of the settlement δ_r by means of

$$\delta_r = s \cdot d_s$$

where $s = \frac{3}{4}$ in this case and in the axi-symmetrical case s is equal to unity.

It seems reasonable to extend the use of such a factor to all cases by means of

$$s = \tfrac{1}{4}\,(3 + B/L) \tag{2.10}$$

where B is the width and L the length of the foundation.

The Conventional Method

After determination of the vertical stress increments, the corresponding deformations are determined on the basis of oedometer tests, and an integration along the vertical centreline gives the settlement.

The deformation properties of a preconsolidated clay depend very much on the in situ overburden-pressure (unloading ratio). It is thus necessary to perform reloading curves at the same pressure as in the corresponding settlement analysis or to use an empirical formula (2.7) for the oedometer strains.

In plate tests the relative modulus-increment α is nearly unity and the theoretical stress distribution approximates the natural stress distribution as closely as possible considering that the soil is not an elastic material.

Since lateral deformations do not occur in the oedometer but exist beneath foundations, the settlement curve develops a wrong shape. Fig. 2.31 shows the mean deformation of five plate tests under equal circumstances and the result of the conventional
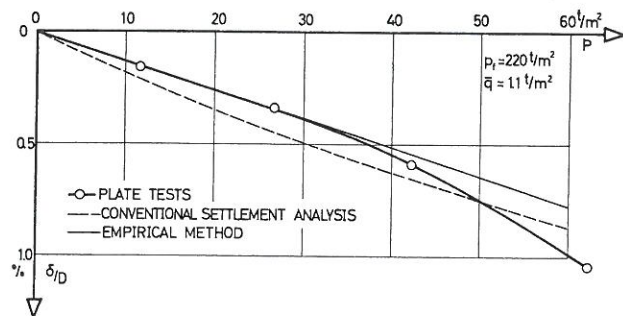

Fig. 2.31 Plate test results compared with settlement analysis.

method based on oedometer test results as expressed by formula (2.7). The deformations are somewhat too large for smaller stresses but too small for higher pressures. It means that even the deformations determined in the new oedometer are too large, probably because the friction causes some difficulties in the statistical treatment of the test results and to some extent caused by deformations between the small filterdisc and the sample. The settlement curve follows the initial tangent for large F_d, where F is the factor of total safety and d denotes the drained state. The suffix u will be used in the undrained state.

41

The Initial Tangent Method

In order to avoid that the calculated settlement curve is upwards concave and to obtain a simple relation between calculated and observed settlements a new empirical method is proposed, in the following called the initial tangent method.

First we will consider the initial tangent of the calculated curve instead of the curve itself. By differentiation of formula (2.7c) we get for $\bar{\sigma} = \bar{\sigma}_u$

$$K_t = \frac{d\bar{\sigma}}{d\varepsilon} = 2.3 \frac{(a+1)\,\bar{\sigma}_u + b}{a'\,\dfrac{e^m}{1+e}} = A\,\bar{\sigma}_u + B$$

After that we can determine a rectilinear settlement curve which also gives too large settlements. But by multiplying these settlements with a constant factor smaller than one it should be possible to calculate the initial tangent of the observed settlement curve, and this seems to give acceptable results for $F_d > 4$.

This factor is determined in all plate tests with a fully known stress level and the result is shown in table 2.7. The mean value of this factor is 0.8 with a standard deviation of 0.05. The settlements of plates are influenced by two important factors. Stones be-

neath the plate give too small settlements and tilting of the plates causes larger settlements. Since it is impossible to take these factors into account all plate tests are used except one test with extremely small settlements (test no. A 5).

In the following this factor will be verified in settlement analysis of three structures.

Settlement Observations

The settlements of three structures on preconsolidated moraine clay were observed and the in situ pressures determined by observations of the ground water level.

These three structures and some properties of the subsoils are shown in fig. 2.32. It can be seen that the surface of the soil has a very complicated shape. The Carlsberg silo is placed in the corner of a large excavation and the Muus silo is situated at the end of pier with canals on three sides. The Ammonia silo seems to have uniform foundation circumstances. Because of these heterogenities the settlements can be expected to be somewhat greater than calculated.

The Carlsberg silo consists of a main building

TABLE 2.7
Settlement analysis of plate tests

Test no.	Surface load t/m²	δ_{obs}	δ_{calc}	obs/calc	Test no.	Surface load t/m²	δ_{obs}	δ_{calc}	obs/calc
MS1	1.95	0.100	0.154	0.65	D2	1.0	0.085	0.190	0.45
A4	2.4	0.108	0.139	0.78	D3	1.0	0.125	0.194	0.65
A5	2.4	0.020	0.139	(0.14)	D4	1.0	0.145	0.194	0.75
A6	2.4	0.066	0.139	0.48	D5	0	0.230	0.232	0.99
A7	2.4	0.270	0.139	1.95	D6	0	0.206	0.232	0.86
B1	2.3	0.148	0.135	1.10	D7	0.7	0.160	0.228	0.70
B2	2.3	0.230	0.135	1.71	D8	0.7	0.138	0.228	0.61
B3	0.9	0.134	0.212	0.63	D9	0.7	0.175	0.228	0.77
B4	0.9	0.170	0.212	0.80	D11	1.1	0.110	0.199	0.55
B5	0.9	0.148	0.212	0.70	D12	0	0.210	0.320	0.66
B6	~ 0	0.400	0.320	1.25	E1	0.2	0.200	0.283	0.71
C1	1.5	0.125	0.162	0.77	F1	0.8	0.066	0.178	0.37
C2	1.5	0.179	0.162	1.10	F3	0	0.192	0.297	0.65
C3	1.1	0.160	0.199	0.80	85	2.35	0.040	0.074	0.54
C4	1.1	0.120	0.199	0.60	86	2.35	0.090	0.074	1.22
C5	1.1	0.185	0.199	0.93	159	0.70	0.050	0.110	0.45
C6	1.1	0.160	0.199	0.80	304	0.70	0.046	0.106	0.43
C7	1.3	0.182	0.186	0.98	305	0.70	0.070	0.106	0.66
C8	1.0	0.155	0.205	0.76	301	0.2	0.400	0.387	1.03
C9	1.3	0.150	0.186	0.81	302	0.2	0.460	0.387	1.19
C11	1.3	0.144	0.186	0.78					
C11	1.3	0.125	0.186	0.67					
C11	0.8	0.220	0.220	1.00					
D1	1.0	0.109	0.190	0.57					

and an access-tower, here treated as two different foundations because of the relatively thin moraine layer, which is assumed to account for all observed deformations. The dimensions of these foundations are $21.6 \cdot 17$ m² and $17.7 \cdot 3.7$ m².

The foundation of the Ammonia silo is circular with a diameter of 12 m. Muus's silo has an area of $28.5 \cdot 23.4$ m².

The consolidation time t_c defined in fig. 3.1 can be estimated by means of Paper 3

Carlsberg's silo	$t_c \sim$	800 hours
Carlsberg's access tower	$t_c \sim$	60 "
Ammonia's silo	$t_c \sim$	350 "
Muus's silo	$t_c \sim$	2000 "

The construction periods are longer than the corresponding consolidation times and therefore drained states sometimes occur. These states are specially marked in fig. 2.33 in which the observations and the results of settlement analysis with initial tangents are shown.

Three of the foundations are treated as circular footings with equal areas. The relative modulus increment is determined by (2.9) and the stress distribution is calculated by means of Boussinesq's formulas and fig. 2.30. The foundation of the access-tower is approximated by a two-dimensional foundation and the shape factor (2.10) is used.

Regarding the black points only it can be concluded that the initial tangent method for small loadings

agrees very well with settlement observations too, being the same result as obtained by plate tests.

The subsoil beneath Muus's silo was investigated to a depth of $Z/D = 0.55$ only, here having constant strength. The underlying strata are probably stronger and stiffer than this soil, but since this has not been investigated, we have to suppose the soil to be homogenous to a great depth, and the calculated settlement is therefore too great.

The two points marked A deviate from the theory, because undrained states cause further deformations. This will be demonstrated later on.

Settlements for $F_d < 4$

The horizontal deformations can be taken into account in a quite empirical way, if we assume that the deviations from the theoretical settlements as determined previously depend on the factor of total safety F_d only.

This function can be found by means of drained plate tests performed on untilted plates and carried on until failure.

By comparing the settlement of a plate with the initial tangent to the settlement curve the relative deviation from this tangent can be determined. The results of 15 drained plate tests form the curve in fig. 2.34. It can be seen that the initial tangent method gives reasonable results for $F_d > 4$, and if $F_d = 2$ the settlement is twice that normally calculated. In the
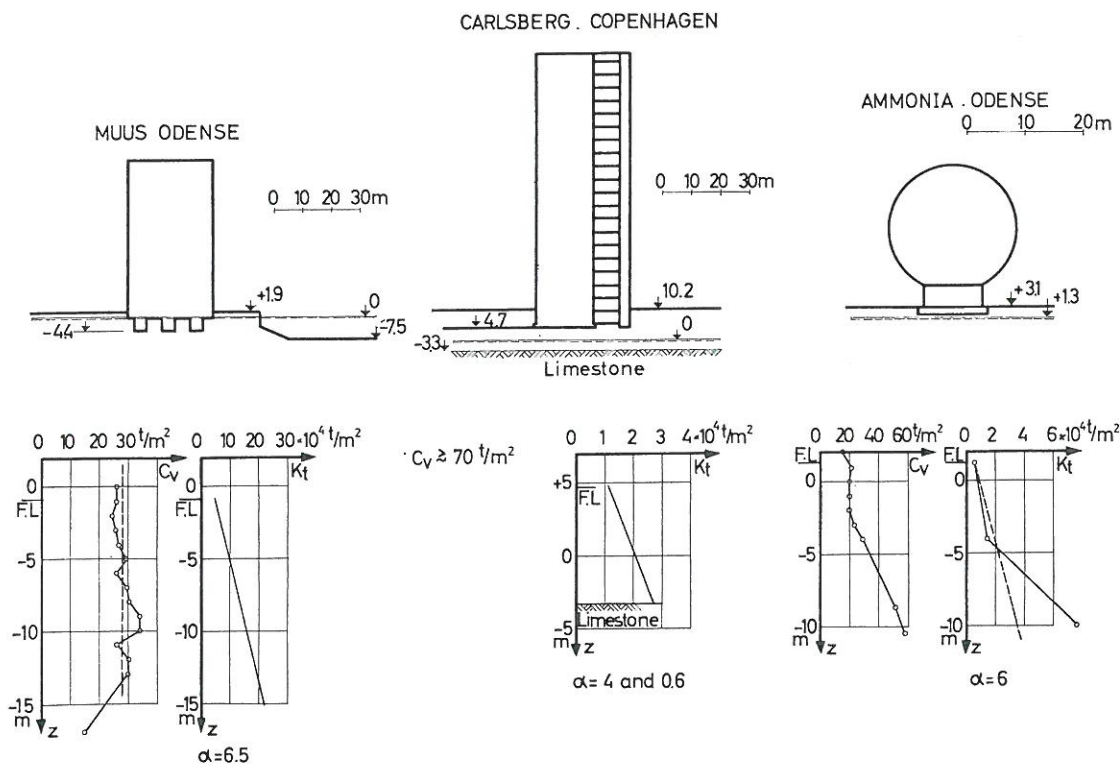

Fig. 2.32 Three structures on moraine clay.

second chapter it is shown that the long term bearing capacity is normally more than twice the short term bearing capacity, and therefore F_d is normally bigger than 4 and the conventional empirical method gives reasonable settlements.

By means of the strength properties given in chapter 2 it is possible to estimate the total safety factor F_d.

The access tower of Carlsberg was always in a nearly drained state. The long term bearing capacity is 470 t/m², the maximum load 77 t/m² and $F_d > 6$. The settlement can be estimated by means of oedometer tests (see also fig. 2.34). This is valid for the

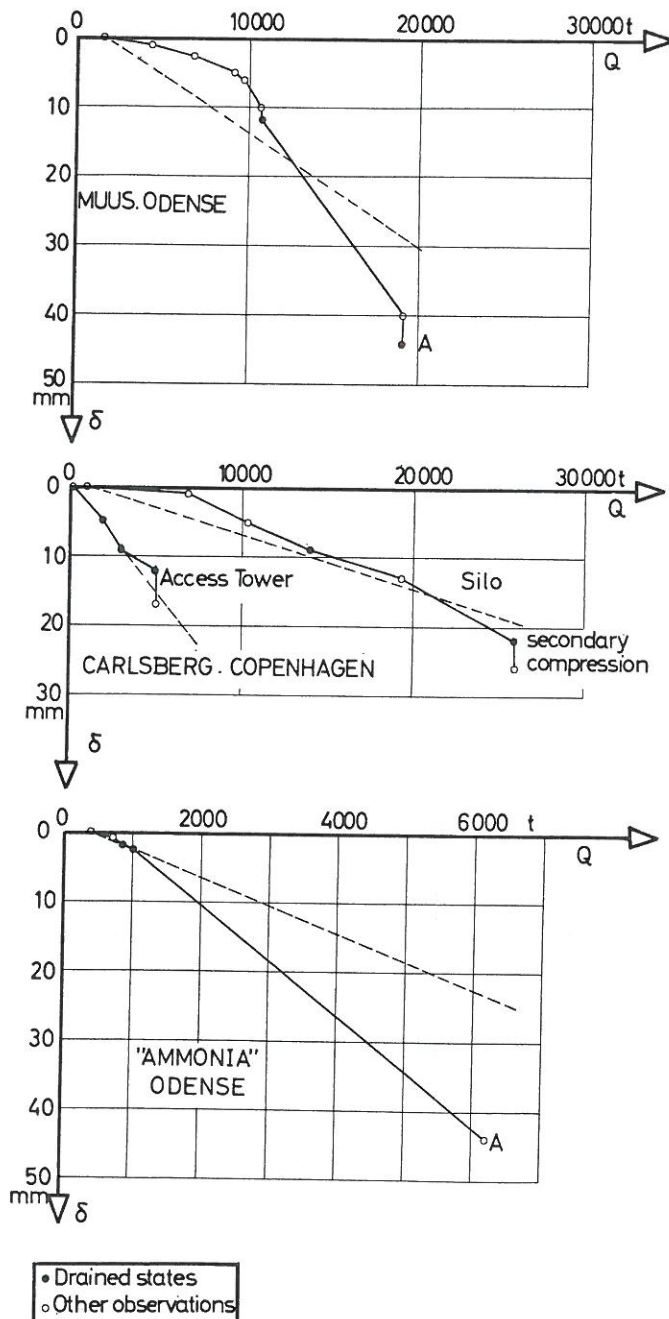main silo too, having a long term bearing capacit greater than 700 t/m², and $F_d > 10$.

The Ammonia silo was built over such a lon period of time that drained states occurred for th dead load, and $F_d > 40$! But by filling the silo witl 5200 t water in 40 hours, an undrained state wa caused and F_u decreased to 2. The long term bearin capacity is nearly 4 times the short term one. ($F_d = 8$). This situation is very complicated, but will here bt treated in a simplified manner. If this foundation wa: loaded very quickly until the undrained failure occur red ($F_u = 1$), the settlements would be very large anc the structure would fall, but if the foundation wa: loaded up to the same pressure so slowly that al settlements were nearly drained, F_d would be ~ 4 and only small settlements could be observed. The settlement also depends on the loading rate for values of F_u bigger than unity, but of course an upper limit for this effect exists.

For the loading in question we got settlements twice as large as that calculated. This corresponds with the curve for the drained plate test (fig. 2.34).

The Muus silo was built up in 3 weeks, and an undrained state occurred with $F_u > 7$. The short term bearing capacity was reduced somewhat because of the canals by means of stability analysis. In this case it was not possible to observe any influence from the loading rate.

For some months the load was nearly constant, but the strength propertiets of soil do not increase considerably during consolidation because the volumetric strains are very small and in some parts of the soil even negative. Here we assumed that the undrained shear strength was constant during loading. 9000 t grain was filled into the silo in 3 weeks and $F_u \sim 3.5$. Since $F_d > 6$ the total settlement should be determined by the dotted line in fig. 2.33. The influence of the undrained state is obvious here, too.
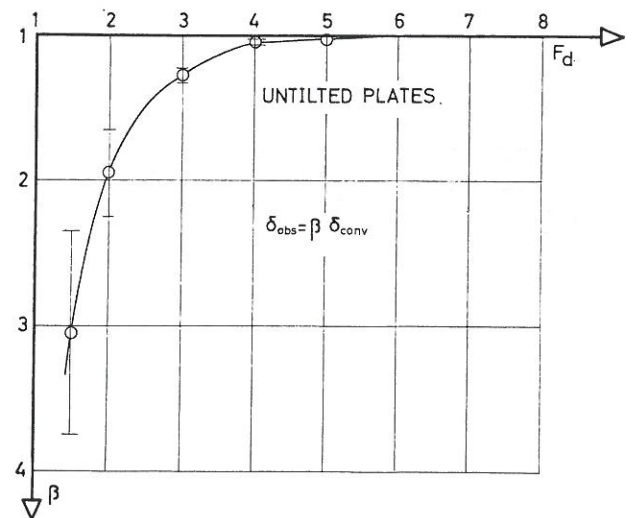

• Drained states
○ Other observations

Fig. 2.33 Settlement observations and calculated settlements. (An example is shown in table 2.8).

Fig. 2.34 The influence of the factor of safety on the settlements of plates.

44

Conclusion

Some methods of settlement analysis were investigated by comparing theoretical settlements with observed ones. The settlement of three structures and 42 drained plate tests was measured.

The theory is based on Boussinesq's formulas for a point load, but due to the increasing stiffness with depth the stresses in the centreline are more concentrated. According to Fröhlich's theory this should for moraine clay give about 10 percent larger settlements of structures but not of small plates. However, this has not been observed to be the case. Other factors influencing the settlements are rigid underlying strata and the depth of the foundation below the surface. These factors seem, however, to be rather unimportant for foundations on moraine clay.

It is shown that the conventional method based on oedometer tests estimates deformations larger than those observed, because some irrelevant deformations occur even in the new oedometer, and because the friction causes some difficulties in the statistical treatment of the test results. But it has been shown that by multiplying the calculated deformations with a factor 0.8 this method gives results coinciding with the tests for very small stresses. By differentiation of the formula for oedometer tests the initial tangent can be determined, and by using this tangent instead of the whole oedometer curve as a first approximation, we obtain reasonable results for $F_d > 4$, where F_d is the factor of total safety. This method has been verified by settlement observations.

If the strength properties of the soil are known, the conventional method can be extended to $F_d < 4$ by multiplying the calculated settlement by a factor depending on F_d. This factor has been determined by means of 15 drained plate tests.

Summary

This paper deals with results obtained in the new laboratory equipment mentioned in Paper 1.

Several moraine clays have been investigated. The void ratio varies between 0.52 and 0.24 and the undrained shear strength c_u takes values between 5 and 70 t/m².

It has been shown that the strength properties $\overline{\varphi}$, $\overline{c}$ and c_u can be expressed as functions of the void ratio and the relative stress level ($\sim \sigma_o/\sigma_{pc}$) only. From these functions it can be concluded that when $e > 0.30$ the short-term bearing capacity nearly equals the cohesion part of the long-term bearing capacity. Consequently the long-term bearing capacity is normally greater. The permeability of moraine clay is so great that undrained states normally do not exist. In the drained state the factor of total safety F is then normally larger than 4.

Deformations measured in oedometer tests and isotropic compression tests have been treated statistically by adjustment by elements.

Settlements measured by means of plate tests performed in the field under drained circumstances show that the settlement curve for $F > 4$ is nearly linear. For $F < 4$ the plate tests may give a correction factor to the initial tangent as a function of F.

A conventional settlement analysis is based on reloading curves in oedometer tests. The initial (unloading) pressures σ_u are here equal to the in situ pressures in the middle of the respective layers. The settlement curve determined in this way has, however, a wrong shape and an initial tangent overestimating the observed settlement by 25 per cent for $F > 4$.

Consequently the most suitable settlement analysis only includes the initial tangent of reloading curves in oedometer tests. After a reduction of the calculated settlements by 25 per cent these settlements equal the observed settlements for $F > 4$.

This method has been checked by settlement observations, which also show, that this method is nearly independent of the void ratio.